

*Citation for published version:*

Atkinson, AL, Baldock, TE, Birrien, F, Callaghan, DP, Nielsen, P, Beuzen, T, Turner, IL, Blenkinsopp, CE & Ranasinghe, R 2018, 'Laboratory investigation of the Bruun Rule and beach response to sea level rise', *Coastal Engineering*, vol. 136, pp. 183-202. <https://doi.org/10.1016/j.coastaleng.2018.03.003>

*DOI:*

[10.1016/j.coastaleng.2018.03.003](https://doi.org/10.1016/j.coastaleng.2018.03.003)

*Publication date:*

2018

*Document Version*

Peer reviewed version

[Link to publication](#)

*Publisher Rights*

CC BY-NC-ND

## University of Bath

**General rights**

Copyright and moral rights for the publications made accessible in the public portal are retained by the authors and/or other copyright owners and it is a condition of accessing publications that users recognise and abide by the legal requirements associated with these rights.

**Take down policy**

If you believe that this document breaches copyright please contact us providing details, and we will remove access to the work immediately and investigate your claim.

# Laboratory investigation of the Bruun Rule and beach response to sea level rise

Alexander L. Atkinson<sup>1\*</sup>, Tom. E. Baldock<sup>1</sup>, Florent Birrien<sup>1</sup>, David P. Callaghan<sup>1</sup>, Peter Nielsen<sup>1</sup>, Tomas Beuzen<sup>2</sup>, Ian L. Turner<sup>2</sup>, Chris E. Blenkinsopp<sup>3</sup>, Roshanka Ranasinghe<sup>1,4,5,6</sup>.

<sup>1</sup> School of Civil Engineering, University of Queensland, St Lucia, QLD, 4072, Australia.

<sup>2</sup> Water Research Laboratory, School of Civil and Environmental Engineering, UNSW Sydney, NSW 2052, Australia.

<sup>3</sup> Water, Environment and Infrastructure Resilience Research Unit, Department of Architecture and Civil Engineering, University of Bath, Bath BA2 7AY, UK.

<sup>4</sup> Department of Water Science and Engineering, UNESCO-IHE, PO Box 3015, 2610 DA Delft, The Netherlands.  
R.Ranasinghe@unesco-ihe.org (Ph: +31 646 843 096)

<sup>5</sup> Water Engineering and Management, Faculty of Engineering Technology, University of Twente, PO Box 217, 7500 AE Enschede, The Netherlands

<sup>6</sup> Harbour, Coastal and Offshore Engineering, Deltares, PO Box 177, 2600 MH Delft, The Netherlands.

## Abstract

Rising sea levels are expected to cause widespread coastal recession over the course of the next century. In this work, new insight into the response of sandy beaches to sea level rise is obtained through a series of comprehensive experiments using monochromatic and random waves in medium scale laboratory wave flumes.~~Beach response to sea level rise is investigated experimentally with monochromatic and random waves in medium scale laboratory wave flumes.~~ Beach profile development from initially planar profiles, and a 2/3 power law profile, exposed to wave conditions that formed barred or bermed profiles and subsequent profile development following rises in water level and the same wave conditions are presented. Experiments assess profile response to a step-change in water level as well as the influence of sediment deposition above the still water level (e.g. overwash). A continuity based profile translation model (PTM) is applied to both idealised and measured shoreface profiles, and is used to predict overwash and deposition volumes above the shoreline. Quantitative agreement with the Bruun Rule (and variants of it) is found for measured shoreline recession for both barred and bermed beach profiles. There is some variability between the profiles at equilibrium at the two different water levels. Under these idealised conditions, deviations between the original Bruun Rule, the modification

29 by Rosati et al. (2013) and the PTM model predictions are of the order of 15% and all these model  
30 predictions are within  $\pm 30\%$  of the observed shoreline recession. Measurements of the recession of  
31 individual contour responses, such as the shoreline, may be subject to local profile variability; therefore,  
32 a measure of the mean recession of the profile is also obtained by averaging the recession of discrete  
33 contours throughout the active profile. The mean recession only requires conservation of volume, not  
34 conservation of profile shape, to be consistent with the Bruun Rule concept, and is found to be in better  
35 agreement with all three model predictions than the recession measured at the shoreline.

36

37       Keywords: Bruun Rule; sea level rise; coastal erosion; equilibrium profiles; sediment transport;  
38 beach morphodynamics

## 39 1. Introduction

40 With the recent increased rates of sea level rise (Hay et al., 2015), potential future shoreface  
41 response to changing water levels are a persistent concern worldwide. There remains a lack of suitably  
42 long-term measurements of shoreface profile change over timescales associated with sea-level-rise,  
43 henceforth *SLR* (Leatherman et al., 2000). As an alternative to obtaining natural or prototype data,  
44 smaller-scale physical models often behave in qualitatively similar ways to prototype beaches and  
45 shorefaces, forming the same characteristic features at a wide range of scales (Hughes, 1993; van Rijn  
46 et al., 2011). Reduced scale modelling can provide valuable information on factors that influence  
47 shoreface responses to *SLR*, such as overwash or onshore transport in deeper water, with the benefits of  
48 a controllable environment and accelerated timescales. Both overwash and onshore transport in deeper  
49 water have recently been proposed as additional mechanisms to be considered alongside the classical  
50 Bruun Rule (Bruun, 1962; Rosati et al., 2013; Dean and Houston, 2016).

51  
52 The term ‘Bruun Rule’ was first coined by Schwartz (1967) as a result of experiments testing  
53 Bruun’s (1962) model. It is perhaps the most well-known and common approach used to predict  
54 shoreline recession under *SLR*. The basis for the Bruun Rule is related to earlier work on natural beach  
55 profiles (Bruun, 1954), which were shown to exhibit a monotonic concave-up mean profile about which  
56 natural beach profiles fluctuate over time. The mean (also commonly referred to as a dynamic  
57 equilibrium) subaqueous profile shape (Figure 1) has the form:

$$h = A(x_{sl} - x)^{2/3} \quad (1)$$

58 for  $x \leq x_{sl}$ , where  $h$  is the water depth, with an origin seaward of the offshore limit of wave influence  
59 ( $h^*$ ),  $x$  is the cross-shore location,  $x_{sl}$  is the still water shoreline location and  $A$  [ $\text{m}^{1/3}$ ] is a scaling  
60 parameter influenced by controls such as sedimentology and wave climate (e.g. Bruun, 1954; Dean,  
61 1991; Short, 1999). The offshore limit is the location where wave driven sediment transport ceases and  
62 the corresponding depth  $h^*$  is a time dependent variable that is expected to increase with time due to the  
63 increased likelihood of larger waves (Hallermeier, 1981); the concept implies that sediment at depths

64 greater than  $h^*$  is essentially unavailable through wave driven processes and this defines the seaward  
65 location of the active profile. Bruun (1962) used this concept and reasoned that if a mean shoreface  
66 profile in dynamic equilibrium with a quasi-steady wave climate is to be maintained relative to the still  
67 water level in the presence of  $SLR$ , sediment can only come from landward of the offshore limit. This  
68 results in a net-seaward sediment transport and a landward shift of the active profile to facilitate raising  
69 the entire active profile by  $SLR$ , leading to the following formula which has become known as the Bruun  
70 Rule:

$$R = SLR \frac{W}{B + h_*} \quad (2)$$

71 where all components have units of length.  $R$  is the recession of the profile (negative values indicating  
72 progradation),  $W$  is the horizontal length of the cross-shore active profile, with an onshore limit typically  
73 corresponding to a berm with a vertical face at the shoreline and horizontal crest, for which,  $B$  is the  
74 berm height above the zero-datum, mean sea level (in the field) or still water level (in the lab). All  
75 parameters are depicted in Figure 1. Figure 1 also demonstrates the coordinate reference system used in  
76 the present work. The cross-shore horizontal origin,  $x = 0$  m, is located seaward of the offshore limit of  
77 profile change, and in the laboratory, it is fixed over the exposed flume bed in the laboratory  
78 experiments. The vertical origin,  $z = 0$  m, is located at the initial water level; therefore, when the water  
79 level rises, the still water level is at the elevation  $z = SLR$ .

80 The Bruun Rule was developed under the assumption of a dynamic equilibrium profile, which is  
81 the long-term mean profile, shaped under a quasi-steady wave climate. To determine the existence and  
82 shape of the dynamic equilibrium profile requires a dataset of regularly measured profiles that captures  
83 the envelope of profile change that occurs with all water level and climate fluctuations (e.g. storms,  
84 spring-neap tides and longer scale climatic atmospheric and oceanic oscillations). Continued profile  
85 monitoring would be required to determine the maintenance of the dynamic equilibrium profile and the  
86 response to  $SLR$ . Thus, while numerous field experiments intended to investigate the applicability of  
87 the Bruun Rule have occurred, given the temporal constraints required to capture the development and  
88 response of the dynamic equilibrium profile, compromises in experimental design are usually required.

89 For example, instead of mean profiles, instantaneous profiles that feature perturbations such as bars and  
90 berms have been used along with proxies for *SLR*, such as rising lake levels (e.g. Hands, 1979), varying  
91 tidal ranges (Schwartz, 1967) and land subsidence (Mimura and Nobuoka, 1995). Even in reduced scale  
92 laboratories, generating a dynamic equilibrium profile as well as assessing its subsequent response to a  
93 slow change in water level would require prohibitively long duration experiments due to the simulation  
94 of a variable wave climate of sufficient complexity and duration. However, the qualitative similarity in  
95 morphological responses and profile development observed at smaller scales may provide useful  
96 insights into natural, prototype profile responses.

97 To date, there has been no published laboratory based experiment on the recession response of  
98 the shoreline (or any other vertical datum) to sea level rise. There has only been one laboratory study  
99 conducted, in which the Bruun Rule was partially assessed using bar-forming, monochromatic waves  
100 in very small scale conditions (Schwartz, 1967). These cases are discussed in more detail in Section 2.  
101 Therefore, further investigation into the applicability of the Bruun Rule on beach profiles shaped by  
102 wave action is warranted. This paper presents the findings of a recent assessment of the original Bruun  
103 Rule, as well as Rosati et al.'s (2013) recent variant, under controlled laboratory conditions at a larger  
104 scale than those of Schwartz (1967), and which include both barred and bermed profile responses. A  
105 new method for assessing the recession of a profile with a constant change in mean water level is also  
106 introduced in the discussion section. Recession of individual contours, such as the still/mean water  
107 shoreline can easily be affected by short-temporal fluctuations with different wave conditions and  
108 natural bar/berm responses of the beach profiles, introducing noise into the dataset which leads to  
109 uncertainty in quantifying the general profile recession. However, if the profile is in a state of dynamic  
110 equilibrium, maintained at each water level, and the limits of the profile change are known, the mean  
111 recession of all contours in the active profile between the depth of closure and the runup limit, relative  
112 to each still water level, should be the recession predicted by Eq. (2). If this is the case, any two  
113 instantaneous profiles separated sufficiently in time, can be used to determine the recession due to *SLR*.

114

115 The paper is organised as follows: Section 2 presents and discusses further background relevant  
116 to the present paper and outlines the recent variants to the original Bruun Rule and key issues to be  
117 investigated. Methodology follows in Section 3, with descriptions of the experimental setup and  
118 analytical techniques, including a description of the new profile translation model applied to different  
119 idealised beach profiles. The experimental results are presented and discussed in Section 4 with some  
120 general discussion provided in Section 5 and concluding remarks given in Section 6. A companion paper  
121 (Beuzen et al., 2017, in review) extends the current work to consider the response of beaches to *SLR* in  
122 the presence of structures.

123

## 124 **2. Background**

### 125 *2.1 Previous assessments of the Bruun Rule*

126 Schwartz performed very small-scale laboratory experiments in a flume with dimensions 2.3 m  
127 length and 1 m width, using fine (0.2mm) sand and small monochromatic waves with heights,  $H$ ,  
128 ranging between  $0.005\text{m} < H < 0.031\text{m}$ . Qualitative agreement with the Bruun Rule was reported as the  
129 profile was observed to rise by values close to the applied rise in water level and shift landward through  
130 apparent seaward net-sediment transport. However, the landward recession and net sediment transport  
131 were not quantified. Schwartz (1967) also conducted field experiments using neap-spring tides as a  
132 proxy for *SLR* and again found qualitative agreement with Bruun Rule predictions, where profiles  
133 responded to the increased tidal range with a reduction in beach volume and raising of the offshore  
134 profile. However, alongshore migrating sand waves added uncertainty to these findings due to  
135 potentially imbalanced longshore sediment transport. Kraus & Larson's (1988) experiment with tide  
136 gave shoreline variations of *ca* 4m in response to a tidal range of 1m which is well below the expected  
137 Bruun rule 'recession' of approximately 15m (the overall slope being *ca* 1/15). This reduction  
138 corresponds to the response time associated with shoreline change that is considerably larger than the  
139 tide period (12.25hours).

140

141 Investigation of the Bruun Rule based on field observations was undertaken by Hands (1979,  
142 1980) on Lake Michigan. Shoreface profiles were monitored during a period of water level rise (approx.  
143 0.08 m/y between 1967 and 1975) and shoreline recession was observed in many places, with erosion  
144 maintaining nearshore profile shapes under rising water levels. Rosen (1979) studied shoreline recession  
145 and application of the Bruun Rule at Chesapeake Bay, and found the rule to be in good agreement with  
146 observed average recession rates. Dubois (1992) questioned the validity of the studies by Rosen (1979)  
147 and Hands (1979, 1980) due to profiles being affected by bluff relief, which is the mass movement of  
148 sediment down a slip face that can occur in the absence of coastal processes (e.g. wind, waves, and  
149 currents). However, Dubois (1992) did find the Bruun Rule to be in good agreement with measured  
150 recession for the beach and nearshore in a region at Lake Michigan that was unaffected by bluff relief.  
151 Dubois (1992) reported that the slope on the offshore side of the outer bar remained unchanged after a  
152 rise in lake level but the nearshore-bar and trough shape was reasonably well maintained and translated  
153 upward by comparable quantities to the water level rise and receded landward by the same amount as  
154 the shoreline, leading him to conclude that the Bruun Rule may only be applicable in the beach and  
155 nearshore zone.

156

157 Rapid land subsidence ( $\Delta z \approx -0.13$  m/y between 1960 and 1970) due to ground water extraction  
158 has also been used as a proxy for *SLR* by Mimura and Nobuoka (1995) on the Japanese coast, who found  
159 predictions from the Bruun Rule to be within the standard deviation of the measured shoreline change  
160 after filtering some noisy shoreline data. Unfortunately, because no subaerial profile data (to provide  
161 berm height and foreshore slope) were available, the writers used values considered to be typical of the  
162 region, so maintenance of profile shape and volumetric continuity was uncertain.

163

## 164 2.2 Recent variants of the Bruun Rule

165 The original Bruun Rule, Eq. (2), is a special case, where the profile shape is two-dimensional  
166 and perfectly maintained relative to the mean water surface, with the shoreline adjoining the subaerial  
167 profile at a square-topped, vertical berm. Of course, there could be a scenario where the profile shape



168 is not maintained, yet the Bruun Rule still provides an accurate measure of shoreline recession due to  
169 the natural variability and sensitivity of the shoreline to a varying wave climate. However, its simplicity  
170 makes it attractive as a predictor for shoreline response to *SLR*, leading to risk of improper use outside  
171 the parameter space upon which it was developed (Bruun, 1988; Cooper and Pilkey, 2004). Typical  
172 scenarios that should be excluded are: (i) beaches undergoing a dynamic-equilibrium shift, resulting in  
173 a changed mean profile slope ( $\frac{W}{B+h_*}$ ), such as with a change in mean wave climate; (ii) beaches where  
174 longshore sediment volumes are unbalanced; and (iii) beaches affected by sources/sinks;  
175 headlands/inlets; or hard structures (such as non-sandy substrata, cliffs or reefs). These limitations have  
176 led to adaptations of the original Bruun Rule, with additional terms to broaden its applicability (e.g.  
177 Stive and Wang, 2003; Thorne and Swift, 2009; Rosati et al., 2013; Dean and Houston, 2016).

178 While *SLR* is expected to result in upward and landward profile translation, it may also induce  
179 changes in the shape of the active profile and associated sediment transport processes. For example,  
180 overwash enhances landward sediment transport across the beach face (Baldock et al., 2008) and  
181 induces changes in the sediment budget. To account for this, additional terms may need to be added to  
182 the Bruun Rule model. Two such recent contributions are those of Rosati et al. (2013) and Dean and  
183 Houston (2016).

#### 184 *Accounting for profile variability above the mean water level*

185 Berms are formed by the deposition and accumulation of sediment near the runup limit and are  
186 common features on accretive shorefaces. To maintain the berm shape with profile translation due to  
187 *SLR*, the region behind the berm at the initial water level must be filled with sediment, which acts as a  
188 sink, increasing the recession needed to maintain a profile relative to the mean water level. Rosati et al.  
189 (2013) presented a modified Bruun Rule with an additive term to account for this, the deposition  
190 volume,  $V_D$  ( $\text{m}^3/\text{m}$ ):

$$R = SLR \frac{W + V_D/SLR}{B + h_*} \quad (3)$$

191 Rosati et al. (2013) note the model is conceptual and acknowledge difficulty in its application in  
192 a predictive sense, which requires quantification of the deposition volume. In the field, the subaerial  
193 profile is often also dependent on aeolian processes; therefore, overwash is just one of potentially  
194 multiple aspects of subaerial shoreface morphodynamics that may affect the recession with profile  
195 translation (Davidson-Arnott, 2005; de Vries et al., 2014). Estimates of sediment overwash volume over  
196 beach berms is technically feasible (Baldock et al., 2008; Figlus et al., 2010) but not applicable at the  
197 timescales associated with profile response to SLR. However, an estimate of deposition volume and  
198 recession may be obtained by applying a profile translation model that maintains the subaerial profile  
199 shape, assuming a state of equilibrium with the prevailing quasi-steady weather and wave climate (e.g.  
200 the new profile translation model introduced later in Section 3.5).

#### 201 *Accounting for other processes resulting in gradual profile variability*

202 Among others, Dean and Houston (2016) provided a Bruun Rule based shoreline change model  
203 that included a suite of additional terms. Along with general terms for sediment sources and sinks and  
204 alongshore transport gradients, Dean and Houston's (2016) model includes a separate term for sediment  
205 introduced from deeper water across an offshore boundary,  $\Phi$ . This requires an offshore limit that is  
206 shallower than that defined by Bruun (1988), i.e.,  $h^*$  in Eq. (2). Dean and Houston (2016) use an annual  
207 closure depth, defined as an estimated depth where, for an average year, "sediment motion was active  
208 to a significant degree", which allows for small but significant sediment transport across the boundary,  
209 given sufficient time. If the limiting depth of profile change is taken at a longer time-scale (e.g. Bruun  
210 1988) the area of onshore transport may be contained within the active profile and so  $\Phi$  may not be  
211 required as an additional term. Nonetheless, the onshore transport given in Dean and Houston's formula  
212 is important in its own right, and is linked to profile steepening described by Rosati et al. (2013).  
213 Onshore transport occurring from deeper to shallower regions should act to offset the recession due to  
214 *SLR*.

215 Dean and Houston (2016) suggest calculating  $\Phi$  at their offshore boundary through application of  
216 measured historic data. As suggested by Rosati et al. (2013) and Dean and Houston (2016), to apply

217 these additional factors an extensive knowledge of the coastal system and processes influencing the  
218 sediment transport and budget is required. In an enclosed laboratory flume environment, these additional  
219 processes either do not occur or are more easily quantified than in the field. At the time of writing, to  
220 the authors' knowledge, there has been no experimental validation of the additional terms presented by  
221 Rosati et al. (2013) or Dean and Houston (2016).

222

### 223 *2.3 Alternative approaches*

224 The response of beach profiles has been assessed using the original concepts of conservation of  
225 the chosen profile shape and volume continuity via simple profile translation models. For example,  
226 Cowell et al. (1992; 1995) developed the Shoreface Translation Model (STM) and adopted an active  
227 profile shape of the form  $h = Ax^m$ . In contrast to the implementation of this formula in Eq. (1), the  $A$   
228 coefficient and  $m$  exponent are adjusted to fit the natural profile being investigated, rather than being  
229 defined by physical parameters associated with the region (Cowell et al. 1995). Once determined, the  
230 translation maintains the profile shape and operates by volumetric continuity. More recently, Patterson  
231 (2013) developed a large-scale translation model also based on volumetric continuity, but differs from  
232 the STM by allowing the representative profile to change with time and with sediment transport being  
233 process driven. Both of these models use an idealised profile shape that corresponds to the long-term  
234 dynamic-equilibrium mean-profile.

235 The Bruun Rule, in the form of Eq. (2), assumes a vertical berm at the shoreline with a horizontal  
236 crest of infinite length (e.g. Figure 1). It is important to note that the entire active profile is being  
237 translated, not just the shoreline, and both the subaqueous shoreface and subaerial beach typically  
238 deviate from such simply shaped profiles, which may affect the sediment budget (Allison and Schwartz,  
239 1981). Natural beach profiles do not closely follow the 2/3-power profile shape, containing  
240 perturbations such as bars, troughs and steps. Others have found compound profiles, introducing a  
241 perturbation at the intersection of the two profiles, to more appropriately represent some mean profile  
242 shapes (e.g. Inman et al., 1993; Patterson and Nielsen, 2016). Thus, it is important to consider profile  
243 shapes that deviate from the monotonic profile of Eq. (1) with respect to net sediment transport

244 occurring during profile response. Many field investigations of profile response to *SLR* have focused on  
245 the shoreline response (Komar et al., 1991). The shoreline is an easily measurable and consequently  
246 attractive state parameter, but its definition is subject to different interpretations (Boak and Turner,  
247 2005), which could result in different measures of recession. To better resolve the recession parameter,  
248  $R$ , it may be useful to consider the entire active profile, given that it is not just the shoreline that recedes.  
249 When applying the Bruun Rule to a monotonic profile described by Eq. (1), the shoreline, berm crest  
250 and possibly an offshore limit are the only features that are easily distinguishable for measurement of  
251 profile recession. Natural profiles, on the other hand, have other features that can be reliably identified,  
252 such as bars, troughs and steps. However, these features of the surf zone can be changeable, so their  
253 feasibility as reliable state indicators in nature is uncertain and while such features may be transient, the  
254 long term mean profile shift, relative to the water surface, should indicate the recession induced by the  
255 *SLR*; this is discussed further in Section 5. Subaerial beach profiles are also variable and typically not  
256 square-topped like Figure 1, which will affect the recession due to variability in the sediment budget  
257 and overtopping accommodation space of the subaerial profile. Therefore, a new translation model that  
258 assumes constant profile shape and volumetric conservation, but which uses a measured profile that  
259 may contain perturbations will be investigated. The profile translation model, henceforth PTM, has been  
260 developed for this purpose, and is presented in Section 3.5.

261 The remainder of the paper investigates profile responses to rising water levels, using a medium-  
262 scale laboratory wave flume. Key issues investigated are: (i) the degree of profile stabilisation under  
263 stationary wave conditions and preservation of the stabilised profile shape after a change in water level  
264 under the same wave conditions; (ii) cross shore sediment redistribution and the bulk and local net-  
265 sediment transport caused by water level changes; (iii) the effects of sediment sources and sinks at both  
266 ends of the active profile; (iv) the response of barred and bermed profiles to water level changes; and  
267 (v) a laboratory assessment of the original Bruun Rule (Bruun, 1962), the recent variant introduced by  
268 Rosati et al (2013) and a simple profile translation model applied to profiles shaped under stationary  
269 wave conditions.

270

### 271 **3. Methodology**

#### 272 *3.1 Wave flumes and instrumentation*

273 Beach profile evolution experiments designed to test the Bruun Rule were performed in a medium  
274 scale wave flume at the University of Queensland (UQ). The flume is 20 m long, 1 m wide and operates  
275 with a water depth between 0.5 m and 0.8 m (Figure 2). Waves were generated by a piston-type wave  
276 maker with active wave absorption enabled. Resistance-type wave gauges were used to measure the  
277 offshore waves over the horizontal bed section of the flume.

#### 278 *Selection of initial beach profile*

279 The 2/3 power profile demonstrated by Bruun (1954) and Dean (1973) are clearly reasonable fits  
280 to some shoreface mean-profiles; however, opinions vary as to the seaward extent of the 2/3-power  
281 profile. Dean's (1977) derivation, using energy dissipation is valid for the breaker region only and some  
282 suggest it only extends as far as the surf zone (Larson, 1988; Dette et al., 2002). However, Bruun's  
283 (1954) original analysis fitted the 2/3-power law to profiles extending beyond the surf zone, to depths  
284 of 15 m. Others have found better fits using compound profile types (e.g. Inman et al., 1993; Patterson  
285 and Nielsen, 2016) and natural profiles can also exhibit near-planar mean profiles. For example, Figure  
286 3a shows multiple profiles taken over 1.5 years from the 'ETA63' transect on the Gold Coast, Australia  
287 (Patterson, 2013). A linear underlying profile exists between -15 m MSL and mean sea level (approx.  
288 0 m MSL) and Figure 3b demonstrates a smaller mean-error (given in the legend) associated with the  
289 planar profile compared with the closest fitting 2/3-power profiles, calculated by varying the  $A$   
290 parameter ( $0.14 \leq A \leq 0.19$ ) in Eq. (1). Interestingly, some of the best-fit profiles in Dean's (1977) study  
291 were also best represented by linear profiles, where  $m = 0$  in Eq. (1).

292 At small scales, beach profiles tend to be steeper (Vellinga, 1982), and it is the experience of the  
293 authors that a 1:10 profile evolves under the available wave conditions to produce both barred and  
294 bermed profile types. Planar starting slopes are useful when trying to achieve comparable starting  
295 conditions between different tests so most of the profiles were initially shaped to a 1:10 planar slope

296 and topped by a wide berm above the runup limit at the back of the beach. However, to investigate  
297 potential differences obtained using a planar and concave initial profile, one experiment (E-3) used a  
298 monotonic power-law profile, shaped according to the form of Eq. (1). The scaling parameter,  $A$ , was  
299 determined by the offshore limit of water depth at the flume bed,  $h_0 = 0.6$  m, and the sandy profile width  
300 from the shoreline to the bed, set at  $x_{sl} = 8$  m, to provide (Riazi and Turker, 2017)  $A = h_0(x_{sl})^{-2/3} =$   
301  $0.15 \text{ m}^{1/3}$ . This is in good general agreement with the expected values of  $A$  based on the grain size  
302 (Dean, 1977). To avoid a vertical sloped berm at the shoreline, a 1:10 planar profile was tangentially  
303 connected to the monotonic profile (Kriebel and Dean, 1993). The profiles developed at each water  
304 level from both the planar and power-law profiles exhibited a good degree of similarity in profile shape  
305 and recession (more detail of the two profile responses are provided in Section 4). Profiles were allowed  
306 to progress toward equilibrium, so the actual starting profile for the response to water level change is  
307 no longer planar, but a profile at equilibrium with the wave climate.

308

309         There remains a further practical consideration for choosing a plane initial or underlying profile,  
310 linked to the choice of depth of closure or the limiting depth used to define  $W$  and  $h^*$  in Eq. (2). There  
311 is some uncertainty in the measurement of the limiting depth but, provided this location is chosen to be  
312 offshore of the true limit, any error in that choice is cancelled out in Eq. (2) with planar profiles. This is  
313 not the case for non-planar profiles. For example, if the offshore limit is chosen further offshore than  
314 the true limit on a profile where the depth varies as  $x^{2/3}$ , the overall beach gradient will be measured as  
315 milder than the true gradient, and application of the Bruun Rule would result in an overestimated  
316 prediction of the recession and *vice versa*. A planar profile is unbiased in this respect for model-data  
317 comparisons of Eq. (2). Profiles were comprised of natural marine beach sand,  $d_{50} \approx 0.28$  mm. Closure  
318 errors in volumetric sediment transport calculations may occur if the sand in the flume is not compacted  
319 sufficiently; in these experiments the sand had been exposed to hundreds of hours of waves prior to the  
320 initial tests. When resetting the planar profile, the redistributed sediment was carefully compacted

321 manually through the entire profile. Thus, only minor compaction closure errors are expected during  
322 the first few profile measurements after wave exposure.

323

324 Early testing found that alongshore non-uniformity may occur in the 1m wide flume, particularly  
325 with monochromatic and accretionary waves, complicating investigation of cross-shore two-  
326 dimensional sediment transport processes. This was found to be mitigated by the addition of two thin  
327 (2 mm) brass plates orientated cross-shore, dividing the upper shoreface and beach into three equal-  
328 width compartments. These dividers extended typically from above the run-up limit into the mid-surf  
329 zone and are self-supporting, inserted vertically into the sand to a sufficient depth to remain buried  
330 during the experiment.

331

332 The laboratory beach profiles were measured using a non-contact laser profiler capable of  
333 measuring both the subaqueous and subaerial profiles from above the water surface with no bed  
334 disturbance and no requirement to drain the flume or change water levels (Atkinson and Baldock, 2016).  
335 Data is obtained at a resolution of 1 mm in both the vertical and horizontal and the accuracy is of order  
336  $\pm 2$  mm and capable of resolving bed ripples and beach scarps. The profiler comprises eight lasers  
337 mounted across the flume on a trolley, aligned to capture multiple cross-shore profiles along the flume  
338 simultaneously by traversing the trolley horizontally along the length of the flume (Figure 2). The mean  
339 profile from all eight lasers was used for all calculations and model comparisons.

340

### 341 *3.2 Wave and water level conditions*

342 Various researchers have attempted to produce empirical formulae to predict beach response to  
343 different wave conditions (e.g. Gourlay, 1968; Sunamura and Horikawa, 1974; Hattori and Kawamatta,  
344 1980); however, there is uncertainty when using any empirical formulae outside of the parameter space  
345 in which it is developed, and many of the predictive formula are developed for use in the field or with  
346 monochromatic waves. Therefore, wave conditions for the present experiments were chosen through

347 experience gained from previous experiments, where distinct barred or bermed profiles were observed  
348 to develop under known conditions (Baldock et al., 2017).

349 An overview of the experimental program is provided in Table 1. A total of six experiments were  
350 conducted, comprising three barred profiles and three bermed profiles. In each case, wave conditions  
351 were held constant to allow the beach to progress toward a stable profile, at which point the water level  
352 was changed and the waves resumed. In a companion paper, Beuzen et al. (2017, in review) conducted  
353 experiments investigating the difference in profile development under a single step water level rise and  
354 multiple, incremental steps, to the same level as the single step. Although the intermediate profile  
355 development differed, the shoreline recession and beach profile at the end of each experiment were near  
356 identical, irrespective of the water level progression. The Bruun Rule, Eq. (2) itself is also independent  
357 of the rate of *SLR*. Therefore, due to time restrictions on operators, for experimental simplicity and  
358 expediency, the experiments detailed in this paper applied a single step change in water level. Beach  
359 profiles were frequently measured during profile development at each water level to assess progression  
360 toward a stable state. For all but experiment A-1, the total change in water level corresponded to half  
361 the incident significant wave height ( $H_{sig}$ ), representing the ratio given by a likely forecast *SLR* of order  
362 0.5 m over the remainder of the century (RCP 8.5, IPCC 2013) relative to an annual mean wave height  
363 (on the Australian East coast) of order 1 m. Of course, the experiments presented here have stationary  
364 wave climates, so the profile response cannot be expected to respond as it does in the field with a variety  
365 of wave conditions and varying water levels, influencing the profile at various depths, however, given  
366 the requirement to choose a constant water level change, this ratio seems as appropriate as any.

367

368 Using monochromatic waves to generate barred profiles tends to develop cross-tank non-  
369 uniformity after very long run times since the constant breakpoint at the bar tends to result in positive  
370 feedback if the bar skews. Initially, monochromatic wave experiments were conducted and found this  
371 to be the case, therefore, due to the high likelihood of profile instability with monochromatic waves on  
372 barred profiles, only random wave experiments were conducted for the barred profile experiments. The  
373 barred profile experiments consisted of three random wave experiments with similar wave conditions,



374 E-1, E-2 and E-3. Note, experiments E-1 and E-1C are the same experiment, with different durations  
375 following the water level rise due to a cyclic morphodynamic response that occurred. Waves at the  
376 initial water level were run for 49 hours for experiment E-1/E-1C to allow sufficient time for profile  
377 development and stabilisation. Experiment E-1C (C for cyclic) contains the full dataset where profile  
378 development continued for 393 hours after water level rise where three cycles of bar generation and  
379 decay were observed. Given the added complexity introduced by the cyclic bar behaviour and  
380 disproportionate run time between the two water levels, an additional analysis on the same data set  
381 (experiment E-1, Table 1) was performed using the initial portion of the dataset, enabling comparison  
382 of the profiles at similar run times at each water level. To avoid a cyclic response during experiment E-  
383 2 and E-3, the test durations were limited to 50 hours at each water level.

384

385 Three experiments investigating bermed profile responses to water level changes were conducted,  
386 consisting of two monochromatic wave experiments with weak (A-1) and strong (A-2) accretion, and  
387 one random wave experiment (A-3, Table 1). Experiment A-1 was conducted as a pilot study prior to  
388 the installation of the laser profiling system and profiles were measured by surveying the profile at  
389 discrete intervals with a horizontal spatial resolution of 0.25 m  $\pm$  5 mm, and a vertical accuracy of  
390 approximately  $\pm$  5 mm.

391

### 392 3.3. *Sediment transport calculations*

393 Considering the framework presented by Bruun (1988), it is apparent that along with measuring  
394 spatial variations of profile parameters (e.g. the location of the shoreline, bar or berm) to assess recession  
395 values, the mode and direction of sediment transport is also important. Obtaining high resolution profile  
396 data allows increased confidence in the calculation of sediment transport rates through volumetric  
397 conservation (e.g. Exner, 1925; Pelnard-Considere, 1956):

$$\frac{\delta q_s}{\delta x} \approx -(1 - p)\delta z \quad (4)$$

398 where  $q_s$  is the net sediment transport (i.e., the volume moved through a cross-section per unit width,  
 399 with units  $m^2$ , positive onshore),  $\delta x$  is the horizontal (cross shore) increment (m),  $p$  is the sediment  
 400 porosity (taken as  $p \approx 0.4$  for sand), and  $\delta z$  is the change in bed elevation (m). Note, usually there is a  
 401 time component associated with  $q_s$ , we have omitted this as a variable since at equilibrium the duration  
 402 of the experiment becomes irrelevant.

403 The local cross shore net sediment transport per unit width,  $q_s(x)$ , is calculated through integration  
 404 of Eq. (4) over the active profile domain between the limiting depth ( $h^* = x_{min}$ ) and the berm height (or  
 405 runup limit) above the still water level ( $B = x_{max}$ ), corresponding to the most landward location of  
 406 observable profile change, to provide:

$$q_s(x) = (1 - p) \int_x^{x_{max}} \delta z dx \quad (5)$$

407 While minimised with high spatial-resolution measurements, closure errors ( $q_s(x_{min}) \neq 0$ , where the  
 408 integration commences from the landward limit,  $x_{max}$ , seaward) in the integration can still occur with  
 409 unaccounted volume missed due to the alongshore spatial separation of the lasers, variable porosity, or  
 410 compaction due to wave action. Closure errors are dealt with following the methodology of Baldock *et*  
 411 *al.* (2011) by uniformly distributing the residual error through the active profile between  $x_{min}$  and  $x_{max}$ .  
 412 Plotted against  $x$ , the output of Eq. (5) highlights areas where volumetric imbalances may be required  
 413 to be considered for implementation of the additional term in Eq. (3), for example, see Section 3.4 and  
 414 Figure 4c, where berm overwash generates a region of net-onshore transport.

415  
 416 A second useful beach profile change and transport parameter, following Baldock *et al.* (2011), is  
 417 the bulk sediment transport,  $Q_s$  ( $m^3$  per unit width) which is determined by integration of Eq. (5):

$$Q_s = \int_{-\infty}^{\infty} q_s(x) dx \quad (6)$$

418 where positive (or negative)  $Q_s$  represents a net shoreward ( $Q_s > 0$ ) or seaward ( $Q_s < 0$ ) motion of  
 419 the sediment volume that comprises the active profile, which has been used to classify the overall profile  
 420 response as erosive ( $Q_s < 0$ ), accretive ( $Q_s > 0$ ) or stable ( $Q_s \approx 0$ ) (Baldock *et al.*, 2011; Jacobsen and

421 Fredsoe, 2014).  $Q_s$  is also equivalent to the horizontal change of the first moment of the beach profile  
422 and does not equal zero unless the onshore and offshore magnitudes of  $q_s(x)$  are equal. Therefore,  $Q_s$   
423 provides an integrated measure of the overall redistribution of sediment, providing the direction by its  
424 sign, relative to the coordinate system. Relative to a given, earlier profile,  $Q_s$  evolves to a constant value,  
425 as the profile progresses toward equilibrium (cf. Jacobsen and Fredsoe, 2014).

426

### 427 *3.4 Model assessment*

428 Three models were assessed for their accuracy in predicting the observed shoreline recession. The  
429 original Bruun Rule (Bruun, 1962) was assessed by measuring the shoreline recession for each  
430 experiment and comparing with the prediction by selecting the profile limits where the profile change  
431 is consistently less than the measurement accuracy of the profiling technique.

432 The recent modification of Rosati et al. (2013) was tested in the same way as the Bruun Rule, with  
433 the additional step of measuring and applying any deposition volume,  $V_D$ , determined by the net  
434 sediment transport (calculated between the initial and final profile at the raised water level) that occurs  
435 at the berm crest of the initial profile,  $x_{berm}$ , and re-introducing the porosity:

$$V_D = \frac{q_s(x_{berm})}{1 - p} \quad (7)$$

436 Finally, a new profile translation model was assessed by comparing the translated initial water level  
437 profile and the measured raised water level profile and respective net-sediment transport curves. The  
438 profile translation model will now be described further.

439

### 440 *3.5 Profile Translation Model*

441 As proposed in the Section 2.3, a new geometric translation model may help to investigate the  
442 response of natural profiles (that may contain perturbations) to sea level rise. This section details the  
443 method of the profile translation model (PTM). The PTM initially raises the active profile by the water  
444 level rise, connecting to the original profile at each end with a vertical line. At this point the volumes  
445 are not conserved between the initial and translated profile, so the raised profile is incrementally shifted

446 landward, always connected by vertical lines to the original profile, until the volumes balance.  
447 Volumetric continuity is determined by integration of the translated and original profiles. The PTM was  
448 tested by applying to some idealised profile shapes, with net transport distributions also calculated.  
449 Figure 4a shows the classic example of the Bruun Rule with a monotonic 2/3-power profile and vertical  
450 berm at the shoreline. This example confirms model behaviour in accordance with the Bruun Rule: only  
451 offshore sediment transport is present, and the new profile is offset in the landward direction. The  
452 sediment from the upper profile facilitates raising the offshore profile, and the recession predicted by  
453 Eq. (2) agrees to within 1% of the value obtained from the PTM. The slight discrepancy is due to the  
454 finite resolution of the model (profile interpolated at  $\delta x = 1$  mm increments). During the incremental  
455 horizontal shift, the algorithm stops at the first instance the volume balance crosses zero, producing a  
456 slightly greater value than that of Eq. (2).

457 Figure 4 also shows three other scenarios (b, c and d). Figure 4b shows the translation applied to  
458 a shoreface with a sloping upper beach face instead of a vertical berm, the net sediment transport curve  
459 again indicates offshore transport only. The recession predicted by the Bruun Rule and PTM are again  
460 near identical, and are greater than the vertical berm scenario, corresponding to a milder active profile  
461 slope. Figure 4c shows the translation applied to the same idealised profile as 4b, but with a berm  
462 inserted onto the beach. In this case onshore transport occurs, leaving a deposition volume landward of  
463 the original berm. Figure 4d shows the PTM applied to one of the ETA63 Gold Coast profiles (Patterson  
464 and Nielsen, 2016) that features a large offshore bar. Both examples containing a perturbation (Figure  
465 4c and 4d) generate localised net onshore transport (indicated by the  $q_s(x)$  curve) following the  
466 translation, near the perturbation.

467 Note that the profile translation for the idealised case with the berm (Figure 4c) generates more  
468 recession than the case without the berm (Figure 4b), which agrees with the concepts of Rosati et al.  
469 (2013). Applying the Bruun Rule, Eq. (1), to the bermed profile in Figure 4c, and taking the landward  
470 extent for the profile width,  $W$ , as the coordinates at the berm crest yields:

471 
$$R = SLR \frac{W}{B + h_*} = 0.41 \text{ m}$$

472 whereas the PTM predicts a recession of 0.48 m (Figure 4c). Calculating the deposition volume using  
473 Eq. (7) ( $q_s(x_{berm}) = 0.024$ , as indicated in Figure 4c) gives  $V_D \approx 0.040 \text{ m}^2$  and inserting into Rosati et al.  
474 (2013)'s Eq. (3) gives:

475 
$$R = SLR \frac{W + V_D/SLR}{B + h_*} = 0.48 \text{ m}$$

476 this agrees with the PTM. These results indicate that the deposition volume requirement may be  
477 predicted using a translation model, and that the predictions from the PTM automatically include the  
478 deposition volume of Rosati et al. (2013) where it occurs.

479

### 480 3.6 Scaling

481 Scale effects are expected in reduced scale physical models (Vellinga, 1982). However, beach  
482 evolution in similar sized laboratory conditions to those in the present study have been compared with  
483 that of much larger scale facilities (Baldock *et al.*, 2011) and found to have exhibited quantitatively  
484 comparable patterns in sediment transport rates for erosive and accretive conditions. Experiments at  
485 both scales also exhibited features that are typical of natural beaches, e.g. formation of scarps, beach  
486 berms, beach steps, breaker bars and troughs. All these features of beach profiles are observed in the  
487 present experiments and therefore the physical model reproduces the classical morphodynamic  
488 responses observed in the field. Additionally, Van Rijn (2011) compared profile development in  
489 laboratories over three different scales and found the shoreline recession to be in good quantitative  
490 agreement between all three scales; however due to finer sand in the smallest scale, the offshore profile  
491 was smoother. The coarser sediment used in the present experiments would be less likely to suffer this  
492 effect so may generate more realistic subaqueous profile shapes. However, the use of sediment size  
493 similar to that of prototype conditions would result in a distortion between horizontal and vertical scales  
494 (Vellinga, 1982), typically producing steeper profiles at smaller scales.

495

496 The principles of the Bruun Rule, geometric similarity and conservation of volume remain true  
497 at laboratory scale. Considering the inevitability of scale effects on local sediment transport, the aim of  
498 the present experiments was to ensure similitude in profile responses. That is, to generate barred or  
499 bermed profiles with similar morphological evolution to that observed in the field. While the present  
500 experiments do not attempt to model any specific beach, the profiles do respond with sufficient  
501 similarity to natural beaches, considering the distortions introduced by the sediment scaling limitations.  
502 For example, taking the barred profile experiment significant wave heights,  $H_s = 0.13$  m and considering  
503 that typical annual average significant wave heights on the Gold Coast, Australia, (which commonly  
504 feature bars, Figure 3) are of the order  $H_s \approx 1$  m, a vertical length scale ratio of  $N_{Lvertical} \approx 8-10$  may be  
505 reasonable. Froude scaling, requires the fall velocity of the sediment to scale with the square root of the  
506 length scale, such that  $N_{ws} = N_{Lvertical}^{0.5} \approx 3$ , which would correspond to a prototype grain size of around  
507 0.8 mm, which is typical on natural beaches with gradients of 1/10 (e.g. Weir et al., 2006). Conversely,  
508 using  $\frac{H\beta_{sz}}{w_s T}$  (where  $w_s$  is the sediment fall velocity and  $\beta_{sz}$  is the surf zone slope) as a similarity parameter  
509 (Hattori and Kawamata, 1980) indicates that if the grainsize does not change between the prototype and  
510 the model, the 1/10 planar initial slope represents a prototype beach with a gradient approximately three  
511 times smaller. Beaches with slopes of 1/30 typically generate longshore bars during intermediate and  
512 erosive events as observed in the present experiments.

513

514 Therefore, given that reduced-scale laboratory profiles: (i) behave with sufficient similarity to  
515 barred and bermed profile responses observed in nature; (ii) respond at reduced time scales; (iii) profile  
516 responses can be quantified with more accuracy and confidence in the absence of longshore processes;  
517 and (iv) are more financially feasible and accessible; it is considered appropriate to be assessing the  
518 qualitative aspects of the beach responses to changing water levels at the scales presented. Therefore,  
519 physical modelling to investigate beach response induced by raised water levels is warranted.

520

521 *3.7 Determining profile stabilisation or equilibrium attainment*

522 Wave conditions in the present research are held constant (stationary for random waves) with  
523 no tidal or seasonal variability so profiles were expected to progress toward a stable *equilibrium* state  
524 that contain perturbations in the form of bars and troughs or berms and steps. Equilibrium is expected  
525 to develop at an exponentially decaying rate of change (Sunamura, 1983), which could result in  
526 prohibitively long experiment durations, and may not hold after certain durations due to oscillations  
527 about some near-equilibrium state. Even in medium scale wave flumes, a true equilibrium may be  
528 unattainable in any reasonable length of time, if at all (cf. Swart, 1974 figures 16, 43 or 44). Therefore,  
529 in the present experiments, determining profile stabilization and/or attainment of equilibrium was  
530 assessed on a case by case basis. The profile development was monitored through changes in state  
531 parameters, such as the location of the shoreline, bar and berm crest, as well as considering sediment  
532 transport rates and broad profile changes. Once the profile was deemed to have stabilised sufficiently  
533 the water level change was implemented and profile development toward a new stable state commenced.  
534 As shown in Figure 5, the shoreline and bar crest locations were observed to stabilise over time. The  
535 net and bulk transport rates often did not reach a zero value, which would be expected if a true  
536 equilibrium profile had occurred. Instead small near-constant rates corresponding to small changes in  
537 profile shape were common long after the shoreline, bar crest and/or step and berm locations had  
538 stabilised; and in these instances, the active profile was also considered to have stabilised sufficiently  
539 to change the water level. For simplicity, we refer to these as profiles at equilibrium, noting the above  
540 caveats. A cyclic process of bar generation and decay was observed in experiment E-1C, after a run  
541 time of approximately 100 hours, after which the definitions of equilibrium become invalid. This cyclic  
542 bar behavior is consistent with observations from other studies (Swart, 1974 figures 43 and 44) and is  
543 discussed further below. Hence, a subjective decision was required to cease a run when a sufficiently  
544 stable profile is achieved prior to the possible triggering of a cyclic mode of evolution.

545

#### 546 **4. Results**

547 This section presents and discusses the results of the experiments. Table 2 provides all onshore  
548 and offshore limits, measured values for the deposition volume,  $V_D$ , in equation (3), and the measured

549 and predicted shoreline recession for each model. Figure 6 shows each predicted recession value against  
550 the observed shoreline recession for each experiment and Figure 7 provides the percentage error  
551 ( $error(\%) = 100 \left( \frac{R_{predicted}}{R_{observed}} - 1 \right)$ ) of each model with respect to the observed shoreline recession for  
552 each experiment.

553 The results are presented as follows. First, the cyclic bar morphodynamic response, following the  
554 water level rise in experiment E-1C will be presented (Figure 8). Following this, the analysis focuses  
555 on barred and bermed profile response (Figures 9-13). Figures 9-13 each contain four plots (a, b, c and  
556 d). (a) shows the profile development for both the initial and raised water levels. Note,  $t = 0$  indicates  
557 the time the water level was raised. Therefore, in these figures, there are two shoreline locations shown  
558 at  $t = 0$  h, corresponding to the final shoreline location at the initial water level and the new shoreline  
559 location at the raised water level. (b) gives the cumulative bulk sediment transport and relative  
560 shoreline progression (relative to the initial shoreline location at the start of the experiment). (c) shows  
561 the initial and final equilibrium profiles at each water level, as well as the results of the PTM. (d)  
562 provides the local net transport distributions ( $q_s(x)$ ) between the initial water level equilibrium profile  
563 and the raised water level equilibrium profile and translated profile. The period at the initial water level  
564 prior to water level rise are indicated by negative time values along the abscissa.

565

#### 566 *4.1 Barred profile experiments*

567 Experiments E-1C, E-1, E-2 and E-3 were conducted to investigate barred profile responses to increased  
568 water levels when forced with random waves.

569

#### 570 *Cyclic bar with random waves E-1C*

571 Figure 8a shows the profile development during the cyclic morphodynamic response at the raised  
572 water level over 393 hours. Figure 8b provides the cumulative bulk sediment transport and relative  
573 shoreline progression (relative to the initial shoreline location at  $t = 0$  h). The cyclic profile response at  
574 the raised water level resulted in sustained losses of sediment offshore, resulting in a gradually receding



575 shoreline, the location of which was under predicted by all three of the tested models (Table 2, Figure  
576 6 and Figure 7). At  $t \approx 65$  h the bar, having been stable for around 30 hours, progressively decayed over  
577 14 hours and the inner bar grew and propagated offshore (Figure 8a). This cyclic bar behaviour was  
578 captured three times before the experiment finished and is discussed further in Section 6. An  
579 investigation into the offshore wave conditions throughout the experiment confirmed that they were  
580 consistent. The shoreline exhibits progradation at certain times, which appear to align with the initial  
581 stages of bar stabilisation. The cumulative bulk transport demonstrates periods of stability  
582 ( $dQ_{s,cumulative}/dt \approx 0$ ) and accretion ( $dQ_{s,cumulative}/dt > 0$ ) within an overall erosive trend ( $dQ_{s,cumulative}/dt$   
583  $< 0$ ). The accretion events appear to occur around times when the bar either stabilises or decays, with  
584 the strongest accretion occurring at the end of the experiment during bar decay.

585 Figure 8c and Figure 8d detail two different profile responses and the net sediment transport. The  
586 left plots show the profile response between  $70 \text{ h} < t < 77 \text{ h}$  when the bar was decaying rapidly. A strong  
587 net-onshore transport component occurs ( $x \approx 11 \text{ m}$ ) as most of the sediment from the bar fills in the  
588 trough, although there is also small offshore transport further seaward, corresponding to the gradual  
589 offshore accumulation. The right plots show the profile response between  $107 \text{ h} < t < 114 \text{ h}$  when the  
590 inner bar was rapidly migrating offshore; at this time, there is almost no onshore transport component.

591  
592 *Common responses of the barred profile experiments*

593 At the initial water level ( $t < 0$  h, Figure 9a and 10a), the bar grows quickly by eroding the initial  
594 profile around the shoreline and nearshore (approx.  $11 \text{ m} < x < 13 \text{ m}$ ) and both the bar and shoreline  
595 stabilise by  $t \approx -20$  h, although a gradual continued offshore movement of sand is typically indicated  
596 by the cumulative  $Q_s$  plot at the end of the initial water level and slight shoreline recession is still  
597 occurring (Figure 9b and 10b). However, given the relative stability compared with changes occurring  
598 between  $-50 \text{ h} < t < -20 \text{ h}$ , the experiments continued with water level rises at this point. Other recent  
599 experiments (Baldock et al., 2017) also found that even with very long run times there may be a small  
600 degree of net sediment motion landward or seaward despite single state profile parameters (e.g.  
601 shoreline and bar crest elevation) appearing stable.

602 Following the water level change, only small (of order of the measurement accuracy) changes  
603 were observed in the profile elevation offshore of the initial bar crest following water level rise, which  
604 agrees with Dubois' (1992) field observations. The PTM tended to predict a lowered profile offshore of  
605 the original bar (Figure 9c and 10c) and onshore transport in the region of the bar (Figure 9d and 10d),  
606 which exhibits qualitative similarity with the translated Gold Coast profile (Figure 4d). However, this  
607 onshore transport was not observed in the experimental data for experiments E-1 and E-2, although E-  
608 3 did exhibit a small amount of net-onshore transport in the bar region. The shape of the final profiles  
609 through the surf zone was often markedly different at the different water levels. The landward  
610 translation of the bar crest was typically less than that of the shoreline, indicating wider surf zones at  
611 the raised water levels, although the crest elevation of the main breaker bar typically translated vertically  
612 by a comparable value to the water level change. Shoreward of the inner bar, the measured and PTM  
613 predicted cross-shore transport patterns,  $q_s(x)$ , were in good agreement, with the additional observed  
614 recession reflected by the greater amount of offshore transport ( $q_s(x) < 0$ ) throughout the upper profile  
615 for experiments E-2 and E-3. While the surf zone profiles remained changeable, profile similarity was  
616 reasonably maintained on the beach face (Figure 9c and 10c) and the shorelines tended to stabilise for  $t$   
617  $> 30$  h (Figure 9b and 10b). Thus, after the initial response to the change in water level and the shoreline  
618 receding due to erosion, little further sediment is required from the upper profile. Instead, the surf zone  
619 sediment is gradually redistributed, which does not significantly influence the shoreline location during  
620 the remaining evolution. For all three barred profile experiments there were only slight differences  
621 between the original Bruun and Rosati et al. (2013) model predictions (Table 2, Figure 6 and Figure 7),  
622 due to none or only a small quantity of sand deposited above the still water level.

623

#### 624 *Experiment E-1*

625 All variants of the Bruun Rule and the PTM predicted the shoreline recession to within 6% (Table  
626 2 and Figure 7). Figure 9 shows the results for experiment E-1. The rate of change for  $Q_s$  also tends to  
627 zero by the end of the experiment ( $t = 44$  h and 51 h). The change in trend for  $Q_s$  around  $t = 30$  h, and  
628 the slight accretive shoreline response, may indicate stabilisation of the overall system. The minor

629 progradation of the shoreline once the new bar had fully developed may be a result of the evolution of  
630 the inner bar, leading to a reduction in wave energy at the shore. There was only a single bar in the final  
631 profile of the initial water level. At the raised water level, a double bar and step profile remained at  
632  $t = 51$  h and the main breaker bar and trough ( $10 \text{ m} < x < 11.5 \text{ m}$ ) were more defined than those at the  
633 initial water level (Figure 9c), with the result that the initial profile shape was not exactly conserved  
634 following the water level increase.

635

#### 636 *Experiment E-2*

637 The original Bruun Rule and Rosati et al.'s (2013) modified version provided slightly closer  
638 predictions than the PTM, but the difference was minimal and all models under predicted the recession  
639 by approximately 25% (Table 2 and Figure 7). Figure 10b-d illustrate the results of the second erosion  
640 experiment, E-2, where the time at each water level was limited to 50 hours. The profile stabilised at  
641 the initial water level around  $t \approx -20$  h with a well-defined two-bar profile, which was a similar  
642 evolution time to Experiment E-1. After the water level rise, continued offshore transport resulted in a  
643 recession that was much greater than the model predictions, with errors that were comparable with the  
644 experiment E-1C (Figures 6 and 7).

645

#### 646 *Experiment E-3*

647 After water level rise, a small amount of deposition above the shoreline resulted in minor  
648 differences between the original Bruun Rule and Rosati et al.'s (2013) modified version, which both  
649 underpredicted the observed shore recession by approximately 13%. The PTM had a slightly greater  
650 underprediction of 16% (Table 2 and Figure 7). Figure 10a-d also details the results of the erosion  
651 experiment where the initial profile was shaped to a monotonic, concave-up profile. Comparably with  
652 experiment E-2, the profile stabilises at the initial water level around  $t \approx -20$  h with a well-defined two-  
653 bar profile (dash-dot blue line, Figure 10c). The cumulative bulk sediment transport appears to have  
654 stabilised to a greater degree than the planar case for this initial profile.

655

## 656 4.2 Bermed profile experiments (A-1 to A-3)

657 Profile stability under monochromatic waves on bermed profiles was achieved using the channel  
658 dividers, therefore regular and random wave experiments are presented. Experiments A-1, A-2 were  
659 forced by monochromatic waves and A-3 was forced by random waves (Table 1).

660

### 661 *Experiment A-1*

662 Figure 11 provides the results of experiment A-1, which resulted in a mild accretive response,  
663 building a small berm through onshore transport of sediment. Rapid profile development and  
664 stabilisation is apparent from the contour plot and plots of the cumulative bulk sediment transport and  
665 relative shoreline position. Due to the low measurement resolution, the calculations of the deposition  
666 volume and the assessment of profile similarity are subject to greater error than for other experiments.  
667 However, the shoreline position was measured accurately. With reference to Figure 6, Figure 7 and  
668 Table 2, the original Bruun Rule under-predicted the shoreline recession by 23%, the Rosati et al. (2013)  
669 model under-predicted shoreline recession by 14%, and the PTM provided the best prediction, with an  
670 under-prediction of 11%. The net sediment transport curve in Figure 11d displays a qualitatively similar  
671 shape to the measured data in the nearshore, but there are deviations further offshore which may be due  
672 to the development of periodic bars, commonly generated by standing waves which are stationary with  
673 monochromatic wave conditions. The predicted deposition volume from the PTM was  $V_D = 0.027 \text{ m}^3/\text{m}$ ,  
674 which is greater than that observed, and would further improve the predictions of Rosati et al. (2013).  
675 There appears to be a slightly wider berm formed at the initial water level and a more pronounced step  
676 in the final raised water level profile, which may account for some of the discrepancies.

677

### 678 *Experiment A-2*

679 Experiment A-2 ran larger waves with a longer period (Table 1) to promote a stronger accretive  
680 response than for Experiment A-1. Figure 12 illustrates the results, where a large, well defined berm  
681 was built by the waves through onshore transport of sediment. The contour plot, temporal variation in  
682 the cumulative  $Q_s$ , and the shoreline position all indicate profile stabilisation and a trend towards

683 equilibrium. The original Bruun Rule under-predicted the shoreline recession by 7%, while the other  
684 models overestimate the recession. Using the measured  $V_D$  (Eq. (7)), the Rosati et al. (2013) model, Eq.  
685 (3), overestimated the observed recession by 7% and the PTM overestimated by 15% (Table 2, Figure  
686 6 and Figure 7). The predicted deposition volume from the PTM was  $V_D = 0.039 \text{ m}^3/\text{m}$ , which is greater  
687 than that observed (Table 2), consistent with the overestimated recession. Much of the translated profile  
688 receded by more than the measured profile but there is a very close similarity between the profiles before  
689 and after the water level rise (Figure 12c). The measured and modelled net sediment transport curves  
690 are in reasonable agreement (Figure 12d), but the magnitudes for the PTM are greater, consistent with  
691 the overestimated recession.

692

### 693 *Experiment A-3*

694 Figure 13 provides the results for the random wave experiment, A-3. The shoreline stabilised for  
695 a period before the water level rise at  $t = 0 \text{ h}$ , but then began accreting slowly around  $t \approx -10 \text{ h}$ , because  
696 of the berm's continued (albeit very slow) growth seaward. Following the raised water level, the  
697 cumulative  $Q_s$  curve and shoreline both stabilise, indicating near equilibrium conditions at the raised  
698 water level from approximately  $t > 30\text{h}$ , with very similar values at  $t \approx 16 \text{ h}$  also. There is also a gradual  
699 loss to offshore deposition, leading to a deeper offshore limit, following the raised water level.

700 The net sediment transport,  $q_s(x)$ , curves between the initial and raised water level profiles show  
701 a greater amount of transport occurring in both directions compared with the translated PTM profile,  
702 corresponding to an increasing berm volume as well as greater losses of sediment offshore, resulting in  
703 the profile lowering around  $x \approx 11 \text{ m}$ . Although there was a substantial onshore transport associated  
704 with the deposition volume, all models over-predicted the shoreline recession (Table 2, Figure 6 and  
705 Figure 7). Due to the deposition volume, the predicted recession by Rosati et al. (2013) (+27%) was  
706 greater than that of the original Bruun Rule (+10%) and the PTM (+17%). The predicted deposition  
707 volume from the PTM was  $V_D = 0.017\text{m}^2$ , half of that observed (Table 2). We propose two possible  
708 reasons for this. Firstly, the profile may not have progressed far enough toward equilibrium by the time  
709 the water level was changed. However, the profile appeared to have stabilised sufficiently by the usual

710 measures (shoreline, step and berm crest locations). Secondly, overtopping enhances landward sediment  
711 transport by reducing the backwash (Baldock et al., 2008) and therefore the presence of the berm at the  
712 outset of the test at the raised water level promotes greater onshore transport than that which would  
713 have occurred on the plane beach. Therefore, exact profile similarity cannot be expected since the  
714 hydrodynamic-morphodynamic feedback is different in the two tests and this factor is expected to be  
715 exacerbated by the random waves, with variable runup limits. This additional transport occurs in the  
716 inner surf zone ( $11 \text{ m} < x < 12 \text{ m}$ ), and while allowing the berm to grow, also feeds the subaerial beach  
717 profile, resulting in less recession than predicted.

718

## 719 **5. Discussion**

720 From the experiments presented, it is clear that the morphodynamic processes leading to profile  
721 change under rising water levels are extremely complex. Even in reduced scale, and with simplified and  
722 controlled laboratory settings, interactions between the hydrodynamics and morphodynamics of mobile  
723 beds results in variable profile responses that can be strongly influenced by many factors. These factors  
724 include, but are not limited to: the rate of water level fluctuations, feedback mechanisms in the near  
725 shore, the presence of berms under random waves, standing waves due to wave reflection, the  
726 underlying/initial profile slope, and wave-boundary interactions. Following the step change in water  
727 level, the initial and intermediate response and development of the profiles to reattain equilibrium are  
728 not representative of a profile developing with a gradual *SLR*. The actual response to *SLR* on natural  
729 beaches is also far more gradual with many other higher-frequency fluctuations occurring at the same  
730 time. Features like the discontinuity in the PTM figures are not present when the water level changes  
731 are gradual, essentially infinitesimal, which may produce the trailing ramp proposed by Kriebel and  
732 Dean (1993). However, as proposed in Sections 1 - 3, the assumptions underpinning the Bruun Rule  
733 should remain valid for any rate of water level rise, and at any scale. Given the evidence that the final  
734 profile at equilibrium does not depend on the rate of water level change (Beuzen et al., 2017, in review),  
735 we assume the final profiles obtained following a step water level rise do represent the *SLR* response.

736

737 The cyclic behaviour observed in E-1C may be due to a slow offshore transport of sediment,  
738 indicated by the offshore accumulation between  $8\text{ m} < x < 10\text{ m}$  (Figure 8). The bar crest elevations  
739 gradually decrease (Figure 14) until the proportion of breaking waves is no longer sufficient to maintain  
740 the bar, triggering the decay (e.g. Wijnberg, 1997). Gradual deepening of the bar crest appears to be a  
741 common occurrence and has also been documented in prototype scale laboratory experiments (Kraus  
742 and Larson, 1988). Baldock et al. (2017) have linked this trigger to the orbital wave velocity over the  
743 bar crest progressively reducing, until the threshold for sheet flow on the bar crest is no longer  
744 maintained. Ripples then form, leading to diffusion of sediment away from the bar crest. Note that this  
745 may not always be the case; bars have also been observed to migrate to a new location with varying  
746 water levels while maintaining their form (e.g. Nielsen & Shimamoto, 2015).

747 The profile response with initially planar starting conditions and a classical concave power-law  
748 profile is very similar (Figure 10c), as are the derived sediment transport distributions. Slightly greater  
749 offshore transport is present for the planar profile case (E-2). This may be due to a greater requirement  
750 for sediment to build the offshore flank of the bar, particularly at the initial water level for the planar  
751 initial condition, and/or decreased wave energy dissipation seaward of the bar over the steeper offshore  
752 slope ( $x < 9\text{ m}$ ), which may also be the cause of the slightly deeper offshore bar crests for Experiment  
753 E-2. Nevertheless, there is good similarity between the profiles at equilibrium for the two experiments  
754 at each water level, providing similar net-transport distribution patterns, as well as very close agreement  
755 in terms of the shoreline recession, which differs by less than 2% ( $R_{shore}$ , Table 2). The difference in the  
756 predicted shoreline recession for E-3 and E-2 are greater than the measured differences, which  
757 highlights the uncertainty introduced when choosing the limiting depth on the non-planar slope.

758

### 759 *5.1 Mean recession of the profile*

760 While the shoreline change models generally underestimate the shoreline recession, the use of a  
761 single beach state parameter to assess the Bruun rule is only robust if the profile shape is conserved  
762 exactly, i.e. small changes in profile shape due to, e.g., bar/berm responses around the waterline will  
763 lead to differences between measurement and predictions even if the overall profile recedes as predicted.

764 To address this issue a global measure of the recession of the profile would be useful. To some extent  
 765 this is provided by the PTM model. However, the PTM still assumes conservation of the profile shape.  
 766 We therefore determine the mean recession,  $R_m$ , of the profile by averaging the recession of the profile  
 767 at discrete, individual contours,  $R(z)$ , between the offshore and onshore limits of profile change

$$768 \quad R_m = \overline{R(z)} = \frac{1}{z_B - z_{h*}} \int_{-\infty}^{\infty} \{x_{t1}(z + SLR) - x_{t0}(z)\} dz$$

769 where subscript  $t1$  and  $t0$  indicates two profiles separated in time. Thus, for varying water levels, the  
 770 contours for each profile are defined relative to the respective still water levels, i.e., the water level  
 771 change ( $SLR$ ) is accounted for. To demonstrate, Figure 15a shows the same translated 2/3-power profile  
 772 response to SLR as that in Figure 4a. Figure 15b shows the  $R(z)$  aligned with the initial water level  
 773 profile. In this example, all contour recessions, the Bruun Rule, the PTM prediction and  $R_m$  are all equal,  
 774 because of the profile shape maintenance.

775 Figure 16 shows the result of applying this analysis to the final profiles at each water level of  
 776 Experiment E-1C, where the shoreline recession at the end of the experiment was much greater as a  
 777 result of the cyclic bar response and continued offshore transport. Figure 16a shows the two profiles  
 778 with bars, but quite different profile shapes through the surf zone. To better visualise the profile  
 779 recession the elevations of the profile at the raised water level were reduced by the water level change  
 780 (0.065 m) to vertically align with the final profile at the initial water level. Figure 16b shows  $R(z)$ , along  
 781 with vertical lines that indicate the mean contour recession,  $R_m$ , the Bruun Rule prediction, the PTM  
 782 prediction and the measured shoreline recession,  $R_{shore}$ . Note that, now the profile shape is not conserved  
 783 at each water level,  $R(z)$  is variable. This is particularly noticeable around elevations  $-0.21 \text{ m} < z < 0 \text{ m}$ .  
 784  $R(z)$  is greater than  $R_m$  above the shoreline (approximately 0.8 m), highly variable around the bar, and  
 785 offshore of the bar  $R(z)$  is less than  $R_m$ .

786  $R_m$  is close to the recession predicted by the PTM and when the profile shape is exactly conserved  
 787 relative to the still water level the two are equal, e.g. Figure 15. Therefore, a difference between the  
 788 PTM prediction and  $R_m$  gives an indication of experimental error. Sources of experimental error may  
 789 be due to lack of equilibration (at either water level), compaction issues, cross-tank non-uniformity, or



790 measurement error. Figure 17 shows the percentage error of each model's predicted recession with  
791 respect to  $R_m$ , for each experiment, where a negative percentage error indicates an under prediction of  
792 the model compared with  $R_m$ . In comparison with Figure 7, the performance remains variable, but the  
793 absolute error is reduced in most cases. Exceptions are Experiment E-1, where the predictions remained  
794 similar, and the Bruun Rule predictions for Experiments A-2 and A-3. The models under predicted  $R_m$   
795 in many cases; a possible reason for this would be if the profiles had not progressed far enough toward  
796 equilibrium at the initial water level. Using the percentage error of the PTM to indicate experimental  
797 uncertainty suggests that both the Bruun (1962) and Rosati et al. (2013) models provided predictions  
798 that were within 5% of the observations for the erosion experiments, accounting for experimental errors.  
799 The predictions from the model of Rosati et al. (2013) were within the expected experimental  
800 uncertainty. Therefore, the inclusion of the overtopping volume improved the prediction, accounting  
801 for the sediment that was transported landward. This is particularly evident for the bermed profile  
802 experiments, where overtopping was more influential.

803       Using a single measure of the profile recession, such as the shoreline or any other contour relative  
804 to the different still water levels, introduces error and is sensitive to profile shape. The mean recession  
805 of the profile, calculated from many contours through the active profile, provides a more robust  
806 measurement of the mean profile response to changes in water level and does not require the profile  
807 shape to be maintained. This method may be applicable to field profiles also, assuming the field profile  
808 can be assumed to be two dimensional (e.g., no longshore net sediment transport gradients). Under these  
809 conditions, conservation of volume requires that the mean recession of the profile in response to a  
810 change in water level should equal the recession of the dynamic-equilibrium mean profile. Therefore,  
811 any two profiles may be used to calculate the mean recession, providing the limits of the active profile  
812 due to cross-shore processes are known. Similar methods may be applicable for other applications, such  
813 as determining longshore transport gradients.

814

815       The additional term in the shoreline change model of Dean and Houston (2016) described in  
816 Section 2.2,  $\Phi$ , which quantifies the volume of sediment introduced into the active profile from seaward

817 of the depth of closure, could not be assessed in the present experiments. In order for there to be a  
818 notional shallower limiting depth, such as the annual limit of change, a non-stationary wave climate is  
819 required to produce variable profiles. This will be investigated in a later paper where further experiments  
820 with falling and rising water levels and a wave climate that cycles between erosive and accretive  
821 conditions are considered, along with the results of nourishment experiments.

822

## 823 **6. Conclusions**

824 The accuracy of the Bruun Rule (Bruun, 1962), Rosati et al.'s (2013) recent variant and a new  
825 profile translation model (PTM) has been assessed using measured profile changes to different water  
826 levels in medium scale laboratory wave flumes. Experiments were performed for both random wave  
827 and monochromatic wave conditions to form barred and bermed profiles. Beach profile data with high  
828 spatial and temporal resolution were obtained using a laser profiler capable of measuring the sub-  
829 aqueous profile from above the water surface, from which sediment transport rates were derived.

830 The comparison of observed and predicted recession values show that as a measure of shoreline  
831 response to rising water levels the original Bruun Rule predicted the shoreline recession to within 25%  
832 (generally under predicting the observations). Rosati et al.'s (2013) Bruun Rule variant exhibited a slight  
833 improvement when the original Bruun Rule under predicted the observations, but resulted in greater  
834 error in some other cases. The PTM was developed to work on measured profiles, accounting for  
835 overwash deposition automatically and performed comparably with the empirical formulas of Bruun  
836 (1962) and Rosati et al. (2013). The recession of discrete contours was calculated across the active  
837 profile to provide a global measure of the mean recession of the profile, and this value was in better  
838 agreement with the recession predicted by all three models, with errors typically reducing to the order  
839 of 10%.

840

## 841 **Acknowledgements**

842 The authors gratefully acknowledge support from the Australian Research Council through an  
843 APA award to Alexander Atkinson and through Discovery grant DP140101302.

844 Roshanka Ranasinghe is supported by the AXA Research fund and the Deltares Harbour, Coastal  
845 and Offshore engineering Research Programme 'Bouwen aan de Kust'.

846

## 847 **References**

848 Allison, H. and Schwartz, M.L. 1981. The Bruun Rule–The relationship of Sea-Level Change to Coastal  
849 Erosion and Deposition. *Proceedings Royal Society Victoria*, 93, pp.87-97.

850 Atkinson, A. and Baldock, T.E. 2016. A high-resolution sub-aerial and sub-aqueous laser based  
851 laboratory beach profile measurement system. *Coastal Engineering*, 107, 28-33.

852 Baldock, T.E., Weir, F. and Hughes, M.G. 2008. Morphodynamic evolution of a coastal lagoon entrance  
853 during swash overwash. *Geomorphology*, 95(3), pp.398-411.

854 Baldock, T. E., Alsina, J. A., Caceres, I., Vicinanza, D., Contestabile, P., Power, H. & Sanchez-Arcilla,  
855 A. 2011. Large-scale experiments on beach profile evolution and surf and swash zone sediment  
856 transport induced by long waves, wave groups and random waves. *Coastal Engineering*, 58,  
857 214-227.

858 Baldock, T. E., Birrien, F., Atkinson, A., Shimamoto, T., Wu, S., Callaghan, D.P., Nielsen, P. 2017.  
859 Hysteresis in the evolution of equilibrium beach profiles under sequences of wave climates -  
860 Part 1; Observations. In review.

861 Beuzen, T., Turner, I. L., Blenkinsopp, C. E., Atkinson, A. L., Baldock, T. E., Flocard, F. 2017. Physical  
862 model study of beach profile evolution by sea level rise in the presence of seawalls. *Submitted*  
863 *for review – this issue*.

864 Boak, E.H. and Turner, I.L., 2005. Shoreline definition and detection: a review. *Journal of coastal*  
865 *research*, pp.688-703.

866 Bruun, P. 1954. Coast erosion and the development of beach profiles, Beach Erosion Board Corps of  
867 Engineers.

- 868 Bruun, P. 1962. Sea-level rise as a cause of shore erosion. *Journal of the Waterways and Harbors*  
869 *Division*. Proceedings of the American Society of Civil Engineers. Pp.117-130.
- 870 Bruun, P. 1988. The Bruun Rule of erosion by sea-level rise: a discussion on large-scale two-and three-  
871 dimensional usages. *Journal of Coastal Research*, pp.627-648.
- 872 Cooper & Pilkey. 2004. Sea-level rise and shoreline retreat: time to abandon the Bruun Rule. *Global*  
873 *and Planetary Change*, 43, 157-171.
- 874 Cowell, P. J., Roy, P. S. & Jones, R. A. 1992. Shoreface translation model: computer simulation of  
875 coastal-sand-body response to sea level rise. *Mathematics and computers in simulation*, 33, 603-  
876 608.
- 877 Cowell, P. J., Roy, P. S. & Jones, R. A. 1995. Simulation of large-scale coastal change using a  
878 morphological behaviour model. *Marine Geology*, 126, 45-61.
- 879 Davidson-Arnott, R.G. 2005. Conceptual model of the effects of sea level rise on sandy coasts. *Journal*  
880 *of Coastal Research*, pp.1166-1172.
- 881 de Vries, S., Arens, S.M., de Schipper, M.A. and Ranasinghe, R. 2014. Aeolian sediment transport on  
882 a beach with a varying sediment supply. *Aeolian Research*, 15, pp.235-244.
- 883 Dean, R.G., 1977. Equilibrium beach profiles: US Atlantic and Gulf coasts. Department of Civil  
884 Engineering and College of Marine Studies, University of Delaware.
- 885 Dean, R.G., 1991. Equilibrium beach profiles: characteristics and applications. *Journal of coastal*  
886 *research*, pp.53-84.
- 887 Dean, R. G. & Houston, J. R. 2016. Determining shoreline response to sea level rise. *Coastal*  
888 *Engineering*, 114, 1-8.
- 889 Dette, H. H., Larson, M., Murphy, J., Newe, J., Peters, K., Reniers, A., Steezel, H., 2002. Application  
890 of prototype flume tests for beach nourishment assessment. *Coastal Engineering* 47. p.137–177
- 891 Dubois, R. N. 1992. A Re-Evaluation of Bruun's Rule and Supporting Evidence. *Journal of Coastal*  
892 *Research*, 8, 618-628.
- 893 Exner, F.M., 1925. Uber die wechselwirkung zwischen wasser und geschiebe in flussen. *Akad. Wiss.*  
894 *Wien Math. Naturwiss. Klasse*, 134(2a), pp.165-204.

- 895 Figlus, J., Kobayashi, N., Gralher, C. and Iranzo, V. 2010. Wave overtopping and overwash of dunes.  
896 *Journal of Waterway, Port, Coastal, and Ocean Engineering*, 137(1), pp.26-33.
- 897 Hands, E. B. 1979. Changes in Rates of Shore Retreat, Lake Michigan, 1967-1976. DTIC Document.
- 898 Hands, E. B. 1980. Prediction of Shore Retreat and Nearshore Profile Adjustments to Rising Water  
899 Levels on the Great Lakes. DTIC Document.
- 900 Hallermeier, R. J. 1981. A profile zonation for seasonal sand beaches from wave climate. *Coastal*  
901 *Engineering*, 4, 253-277.
- 902 Hattori, M. and Kawamata, R., 1980. Onshore-offshore transport and beach profile change. In *Coastal*  
903 *Engineering 1980* (pp. 1175-1193).
- 904 Hay, C.C., Morrow, E., Kopp, R.E. and Mitrovica, J.X. 2015. Probabilistic reanalysis of twentieth-  
905 century sea-level rise. *Nature*, 517(7535), pp.481-484.
- 906 Hughes, S.A. 1993. Physical models and laboratory techniques in coastal engineering (Vol. 7). World  
907 Scientific.
- 908 Inman, D.L., Elwany, M.H. and Jenkins, S.A. 1993. Shorerise and bar-berm profiles on ocean beaches.  
909 Scripps Institution of Oceanography.
- 910 IPCC. 2013: Summary for Policymakers. In: *Climate Change 2013: The Physical Science Basis.*  
911 *Contribution of Working Group I to the Fifth Assessment Report of the Intergovernmental Panel*  
912 *on Climate Change* [Stocker, T.F., D. Qin, G.-K. Plattner, M. Tignor, S.K. Allen, J. Boschung,  
913 A. Nauels, Y. Xia, V. Bex and P.M. Midgley (eds.)]. Cambridge University Press, Cambridge,  
914 United Kingdom and New York, NY, USA.
- 915 Jacobsen, N. & Fredsoe, J. 2014. Cross-Shore Redistribution of Nourished Sand near a Breaker Bar.  
916 *Journal of Waterway, Port, Coastal, and Ocean Engineering*, 140, 125-134.
- 917 Komar, P.D., Lanfredi, N., Baba, M., Dean, R.G., Dyer, K., Healy, T., Ibe, A.C., Terwindt, J.H.J. and  
918 Thom, B.G. 1991. The response of beaches to sea-level changes-a review of predictive models.  
919 *Journal of Coastal Research*, 7(3), pp.895-921.
- 920 Kraus, N.C. and Larson, M. 1988. Beach profile change measured in the tank for large waves 1956-  
921 1957 and 1962 (No. CERC-88-6). Coastal Engineering Research Center Vicksburg MS

922 Kriebel, D.L. and Dean, R.G., 1993. Convolution method for time-dependent beach-profile response.  
923 Journal of Waterway, Port, Coastal, and Ocean Engineering, 119(2), pp.204-226.

924 Larson, M., 1988. Quantification of beach profile change. PhD. Thesis, Lund University (Sweden) Dept.  
925 of water resources engineering.

926 Leatherman, S.P., Zhang, K. and Douglas, B.C. 2000. Sea level rise shown to drive coastal erosion. Eos,  
927 Transactions *American Geophysical Union*, 81(6), pp.55-57.

928 Ludka, B.C., Guza, R.T., O'Reilly, W.C. and Yates, M.L. 2015. Field evidence of beach profile  
929 evolution toward equilibrium. *Journal of Geophysical Research: Oceans*, 120(11), pp.7574-  
930 7597.

931 Mimura, N. & Nobuoka, H. 1995. Verification of the Bruun Rule for the estimation of shoreline retreat  
932 caused by sea-level rise. *Coastal Dynamics 95*. ASCE, 607-616.

933 Nielsen, P. and Shimamoto, T. 2015. Bar response to tides under regular waves. *Coastal Engineering*,  
934 106, pp.1-3.

935 Patterson, D. C. 2013. Modelling as an aid to understand the evolution of Australia's central east coast  
936 in response to late Pleistocene-Holocene and future sea level change. PhD, University of  
937 Queensland.

938 Patterson, D. & Nielsen, P. 2016. Depth, bed slope and wave climate dependence of long term average  
939 sand transport across the lower shoreface. *Coastal Engineering*, 117, 113-125.

940 Pelnard-Considere, R., 1956. Essai de theorie de l'evolution des formes de rivage en plages de sable et  
941 de galets. Les Energies de la Mer: Compte Rendu Des Quatriemes Journees de L'hydraulique,  
942 Paris 13, 14 and 15 Juin 1956; Question III, rapport 1, 74-1-10.

943 Riazi, A. and Türker, U., 2017. Equilibrium beach profiles: erosion and accretion balanced approach.  
944 Water and Environment Journal.

945 Rosati, J., Dean, R. & Walton, T. 2013. The Modified Bruun Rule Extended for Landward Transport.  
946 *Marine Geology*, 340, 71-81.

- 947 Rosen, P. 1979. An application of the Bruun Rule in the Chesapeake Bay. Proceedings of the Per Bruun  
948 Symposium. International Geographical Union, Commission on the Coastal Environment, 1979.  
949 Newport, RI, USA, 55-62.
- 950 Schwartz, M. L. 1967. The Bruun theory of sea-level rise as a cause of shore erosion. *The Journal of*  
951 *Geology*, 76-92.
- 952 Short, A.D. 1999. Handbook of beach and shoreface morphodynamics. John Wiley & Sons.
- 953 Stive, M. J. F. & Wang, Z. B. 2003. Chapter 13, Morphodynamic modeling of tidal basins and coastal  
954 inlets. Elsevier B.V.
- 955 Sunamura, T. 1983. A predictive model for shoreline changes on natural beaches caused by storm and  
956 post-storm waves, *Transactions, Japanese Geomorphological Union*, Vol.4, 1, 1-10.
- 957 Swart, D.H. 1974. Offshore sediment transport and equilibrium beach profiles (Doctoral dissertation,  
958 TU Delft, Delft University of Technology).
- 959 Thorne, J. & Swift, D. 2009. Sedimentation on continental margins, II: application of the regime  
960 concept. *Shelf Sand and Sandstone Bodies*. Oxford: Blackwell, 33-58.
- 961 Van Rijn, L.C., Tonnon, P.K., Sánchez-Arcilla, A., Cáceres, I. and Grüne, J. 2011. Scaling laws for  
962 beach and dune erosion processes. *Coastal Engineering*, 58(7), pp.623-636.
- 963 Vellinga, P. 1982. Beach and dune erosion during storm surges. *Coastal Engineering*, 6(4), pp.361-387.
- 964 Wijnberg, K.M. 1996. On the systematic offshore decay of breaker bars. *Coastal Engineering 1996*,  
965 3600-3613.

967 Table 1: Summary of experiments detailing Experiment type, ID, profile type (barred or bermed), significant wave height ( $H_{sig}$ ), peak wave period ( $T_p$ ), water level rise ( $SLR$ ) and  
 968 total run times at each water level. Under Profile type M indicates monochromatic waves P is a Pierson-Moskowitz wave spectrum and J is a Jonswap spectrum ( $\gamma = 3.3$ ). \* denotes  
 969 regular wave height,  $H$ , and constant period,  $T$ , for the monochromatic wave cases, instead of  $H_{sig}$  and  $T_p$ .

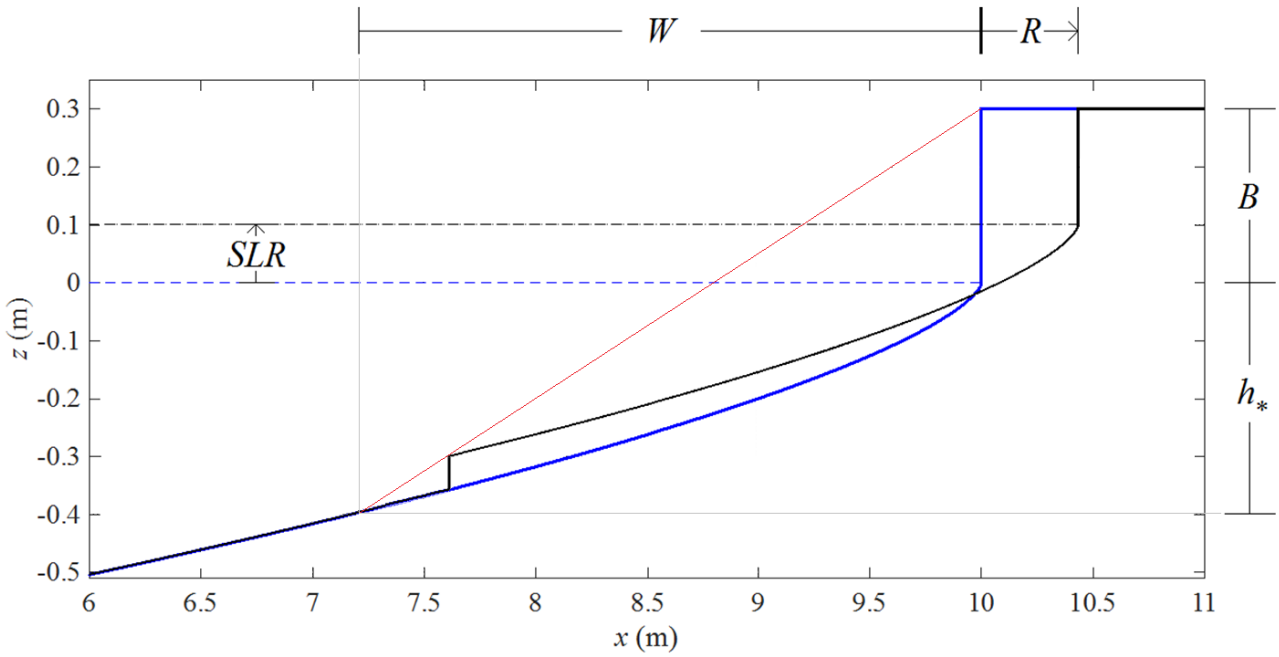
Experiment	ID	Profile type	$H_{sig}$	$T_p$	$SLR$	Time at initial water level	Time at raised water level
			(m)	(s)	(m)	(h)	(h)
Cyclic Bar	E-1C	Bar (P)	0.13	1.20	0.065	49	393
Barred/Erosion	E-1	Bar (P)	0.13	1.20	0.065	49	56
Barred/Erosion	E-2	Bar (J)	0.13	1.20	0.065	50	50
Barred/Erosion	E-3	Bar (J)	0.13	1.20	0.065	54	50
Weak Accretion	A-1	Berm (M)	0.06*	1.50*	0.050	12	12
Strong Accretion	A-2	Berm (M)	0.07*	2.00*	0.035	12	12
Random Accretion	A-3	Berm (P)	0.10	2.00	0.035	41	40



971 Table 2: ID, Bruun Rule parameters ( $SLR$ ,  $h^*$ ,  $B$  and  $W$ ), observed shoreline recession ( $R_{shore}$ ), observed mean contour recession ( $R_m$ ) and recession predictions,  $R$ , for the original  
 972 Bruun Rule (Bruun), the translation model (PTM), and Rosati et al.'s (2013) model (R13). Percentage error ( $\%Error$ ) is provided next to each model's prediction compared with the  
 973 observed, depicted in Figure 9.

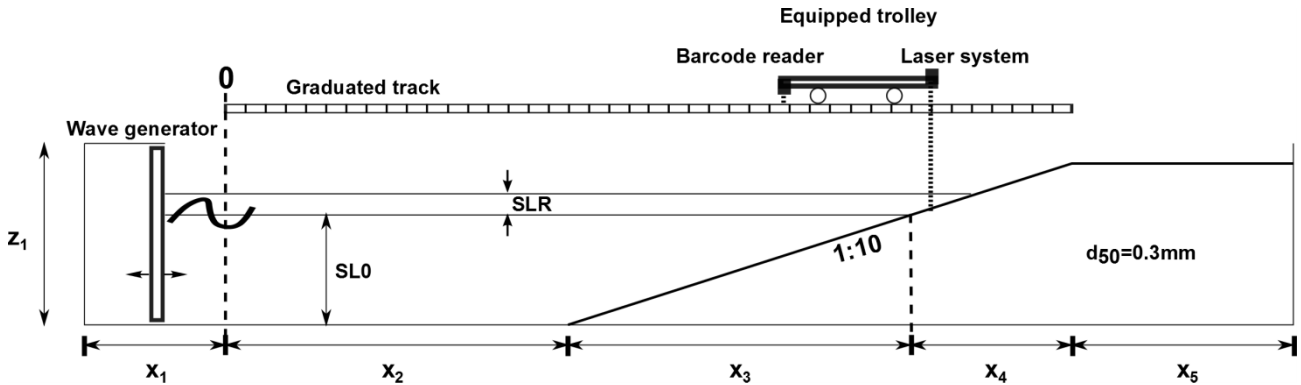
ID	$SLR$	$R_{shore}$	$R_m$	Bruun						PTM		R13		
				$h^*$	$B$	$W$	$\beta$	$R$	$\%Error$	$R$	$\%Error$	$V_D$	$R$	$\%Error$
[-]	[m]	[m]	[m]	[m]	[m]	[m]	[-]	[m]	[%]	[m]	[%]	[m <sup>3</sup> /m]	[m]	[%]
E-1C	0.065	0.869	0.758	-0.575	0.094	6.803	0.098	0.661	-23.9	0.689	-20.7	0.0007	0.662	-23.8
E-1	0.065	0.696	0.706	-0.575	0.094	6.803	0.098	0.661	-5.0	0.689	-1.0	0.0017	0.664	-4.7
E-2	0.065	0.883	0.698	-0.495	0.100	6.087	0.098	0.665	-24.7	0.663	-24.9	0.0005	0.666	-24.6
E-3	0.065	0.870	0.750	-0.409	0.092	5.830	0.086	0.756	-13.1	0.731	-16.0	0.0000	0.756	-13.1
A-1	0.05	0.553	0.522	-0.383	0.045	3.651	0.117	0.427	-22.9	0.490	-11.4	0.0202	0.474	-14.3
A-2	0.035	0.312	0.328	-0.476	0.148	5.191	0.120	0.291	-6.7	0.358	14.7	0.0273	0.335	7.3
A-3	0.035	0.307	0.381	-0.462	0.162	5.999	0.104	0.336	9.6	0.360	17.3	0.0341	0.391	27.4

974  
975



976

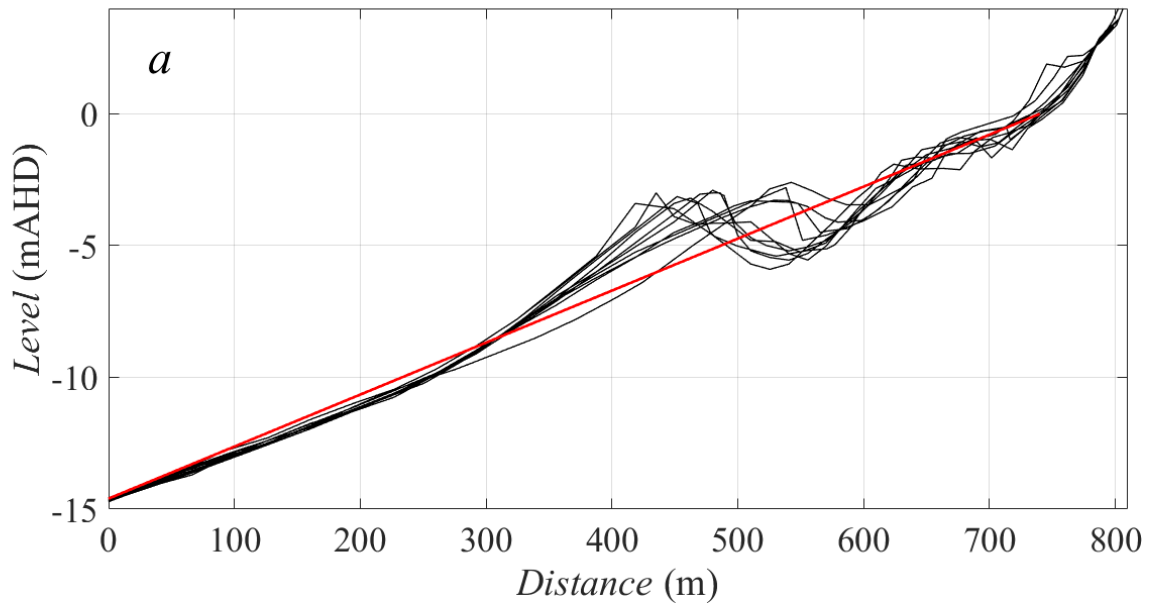
977 Figure 1: Bruun rule profile response and framework applied to an idealised profile with offshore shape  
 978 corresponding to Eq. (1). The red line indicates the slope of the dynamic equilibrium active profile,  
 979 between the offshore limit and berm crest. The  $z$ -axis origin is at the initial water level (blue line), the  
 980  $x$ -axis origin is located off the plot, seaward of the offshore limit of the profile at the initial water level  
 981  $(x, z) = (7.2 \text{ m}, -0.4 \text{ m})$ .



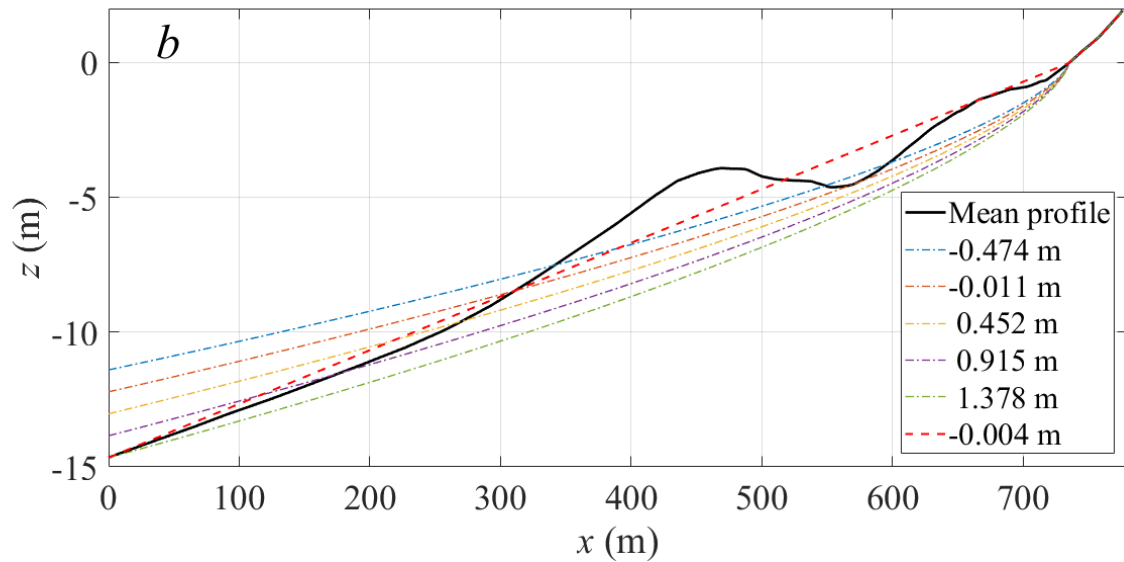
982

983 Figure 2: Wave flume and instrumentation schematic ( $x_1 \approx 3 \text{ m}$ ;  $x_2 \approx 7 \text{ m}$ ;  $x_3 \approx 6 \text{ m}$ ;  $x_4 \approx 2 \text{ m}$ ;  $x_5 \approx 2 \text{ m}$ ;  
 984  $z_1 = 1 \text{ m}$ ).

985



986



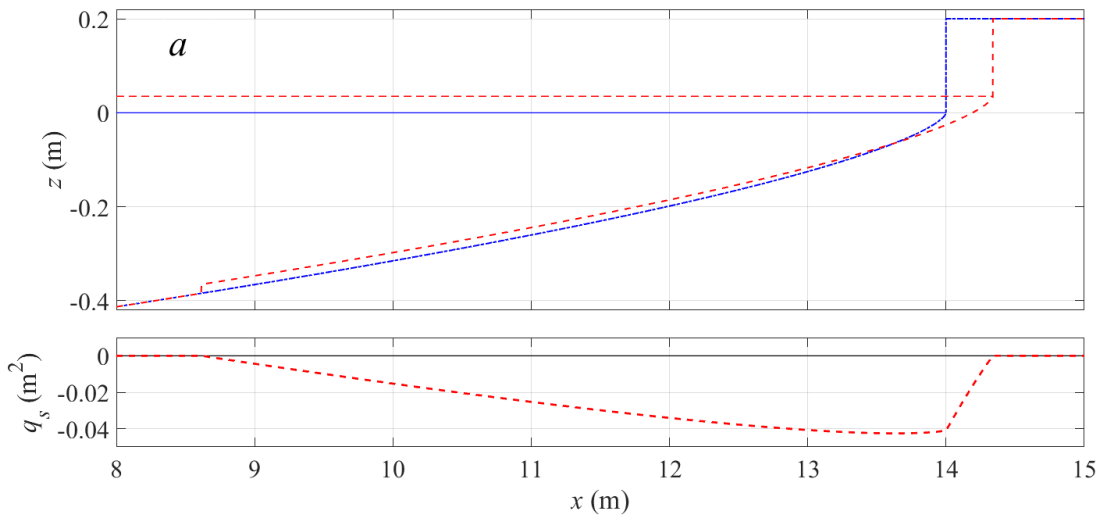
987

988 Figure 3: a) Profiles of a beach at the Gold Coast, Australia (ETA 63) with multiple measurements  
 989 taken over approximately 1.5 years, with best fit planar profile shown in red. b) 2/3 power law profiles  
 990 plotted for a range of  $A$  values ( $0.14 \leq A \leq 0.18$ ) together with the planar profile, red, and the mean of  
 991 the measured profiles (black). The legend shows the mean error of the vertical difference between the  
 992 mean profile and the idealised profiles. Profile data from Patterson (2013)

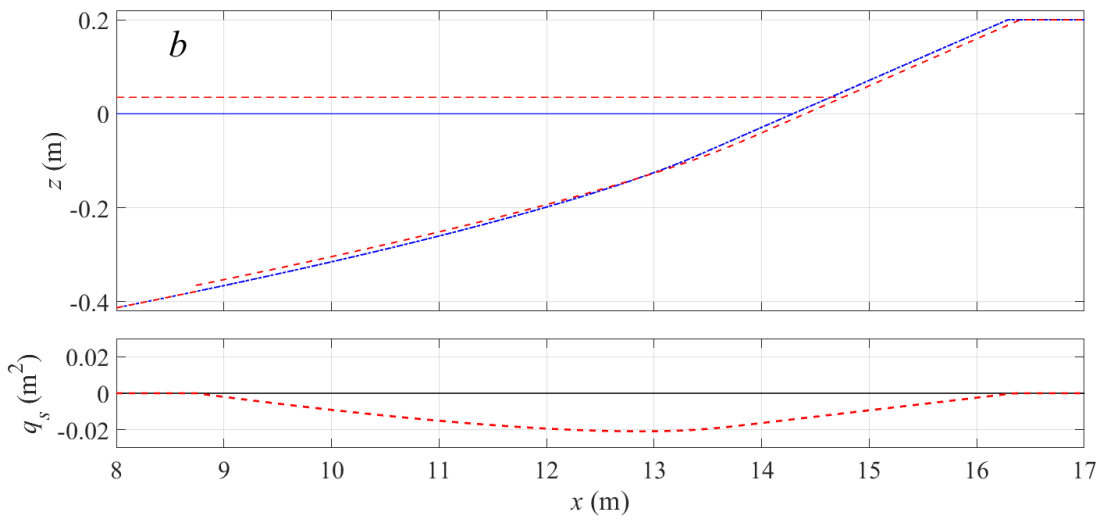
993

994

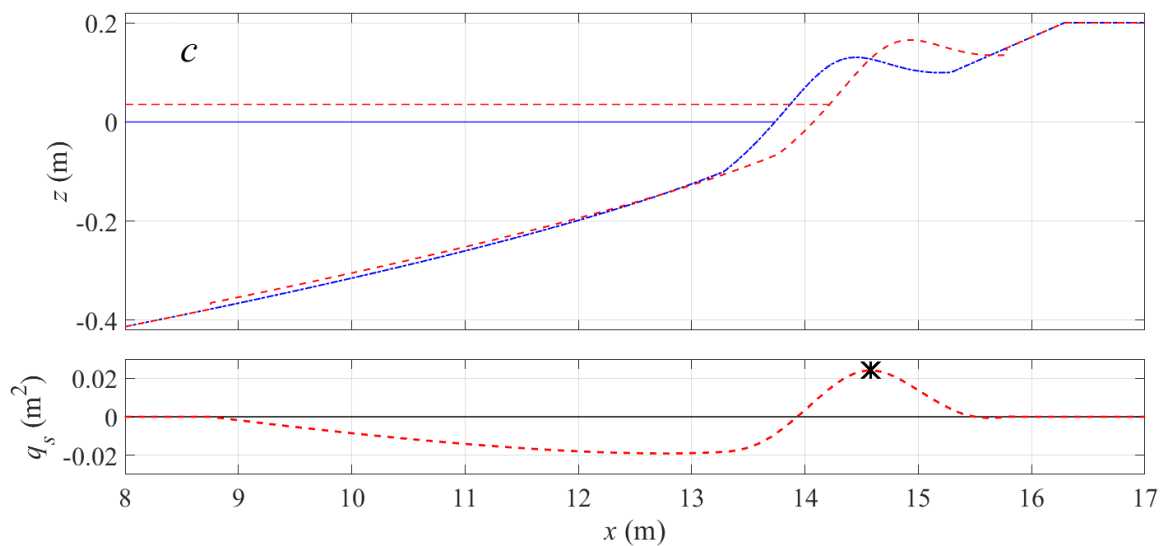
995



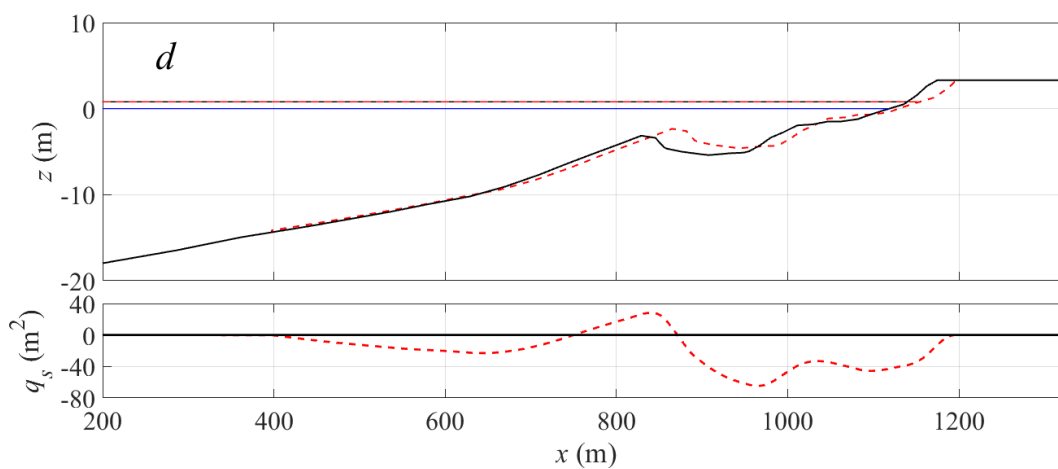
996



997



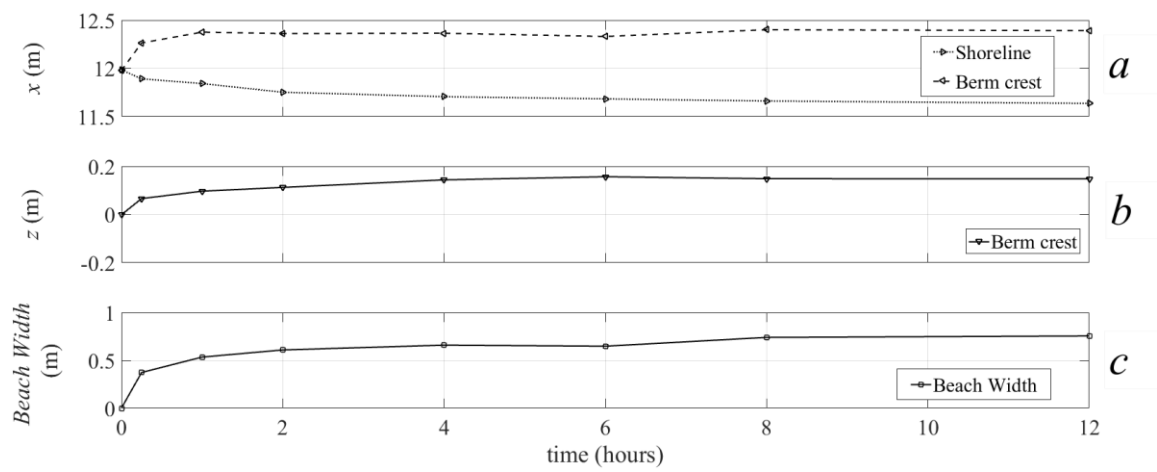
998



999

1000 Figure 4: Profile Translation Model results (top panels) and corresponding net-sediment transport  
 1001 curves (offshore transport when  $q_s < 0$ ) in the lower panels for: a) classical Bruun-type power-law  
 1002 profile; b) power-law profile spliced to a plane sloping upper beach (cf. Kriebel and Dean, 1993); c)  
 1003 power-law profile with berm on upper beach (note the black star on the  $q_s(x)$  plot indicates the net-  
 1004 sediment overtopping,  $q_s(x_{berm}) = 0.024 \text{ m}^2$ ); and d) ETA63 Dec 1988 Gold Coast Profile with the berm  
 1005 crest extrapolated landward.

1006



1007

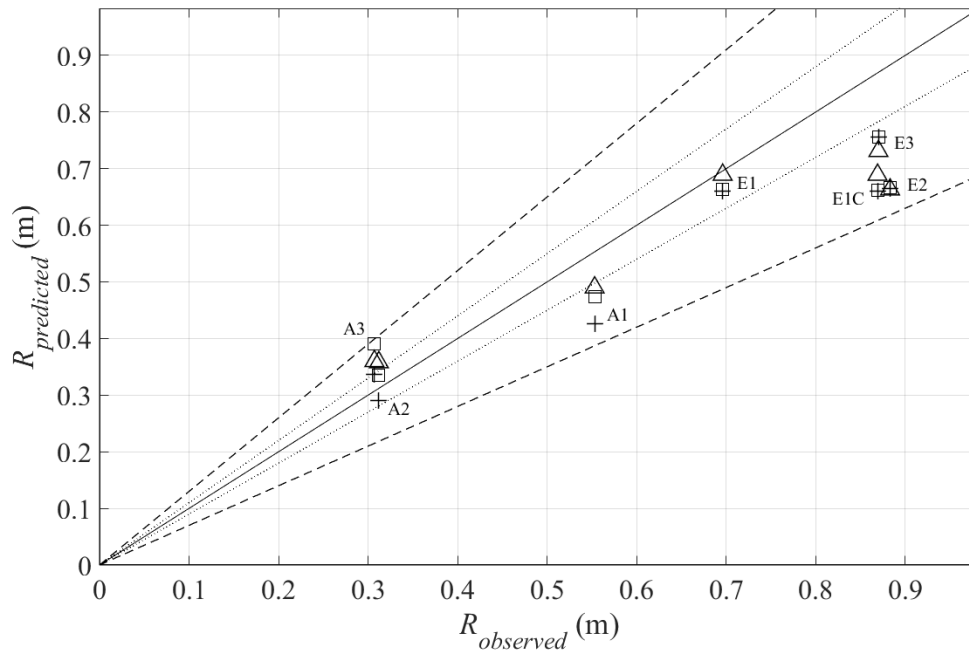
1008

1009

1010

Figure 5: Evolution of profile parameters over time for experiment A-2. a) Shoreline and berm crest horizontal coordinate location, b) berm crest elevation and c) beach width ( $x_{berm} - x_{shoreline}$ ).

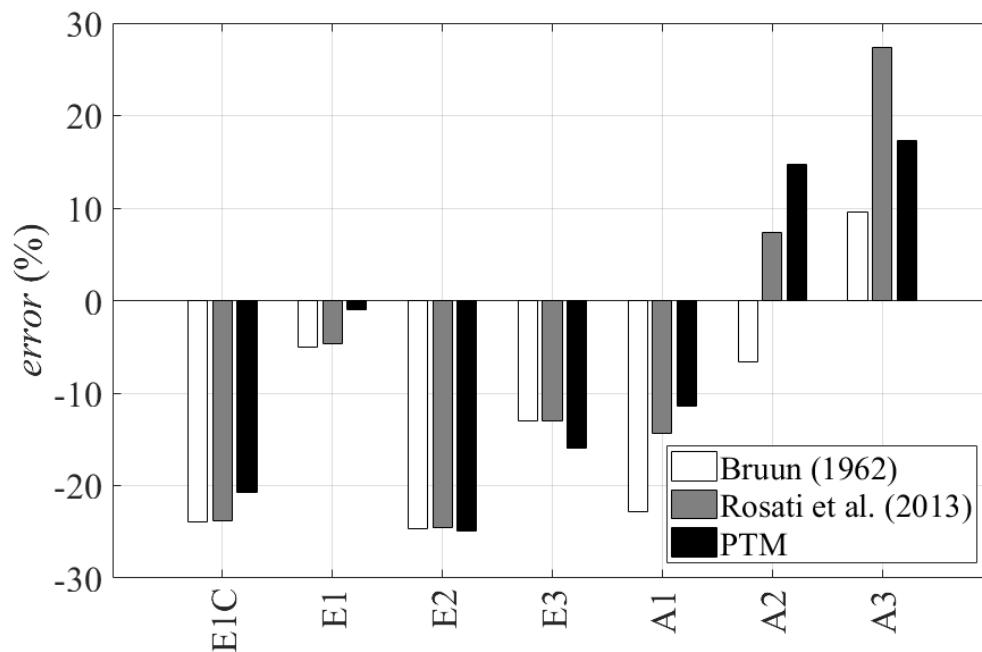
1011



1012

1013

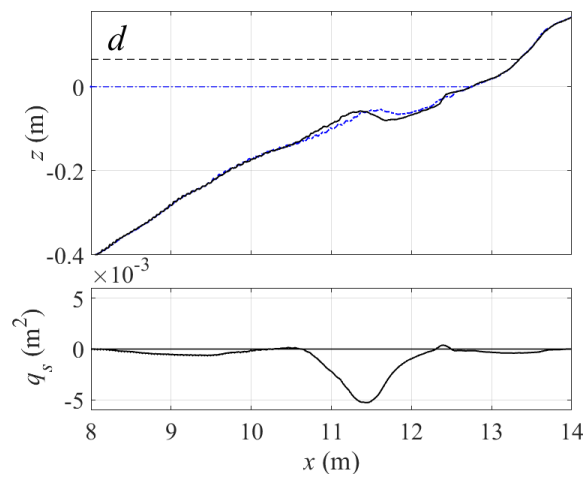
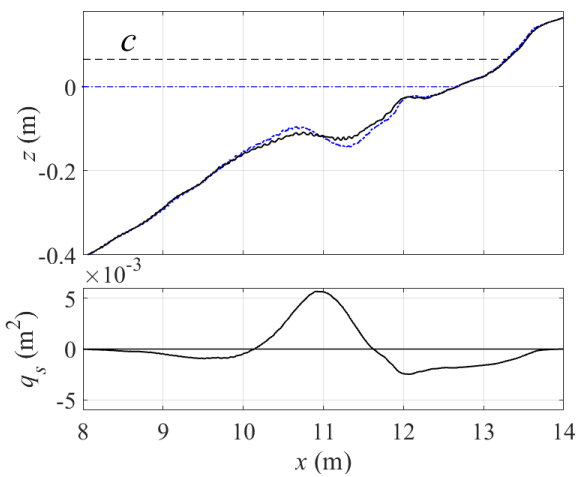
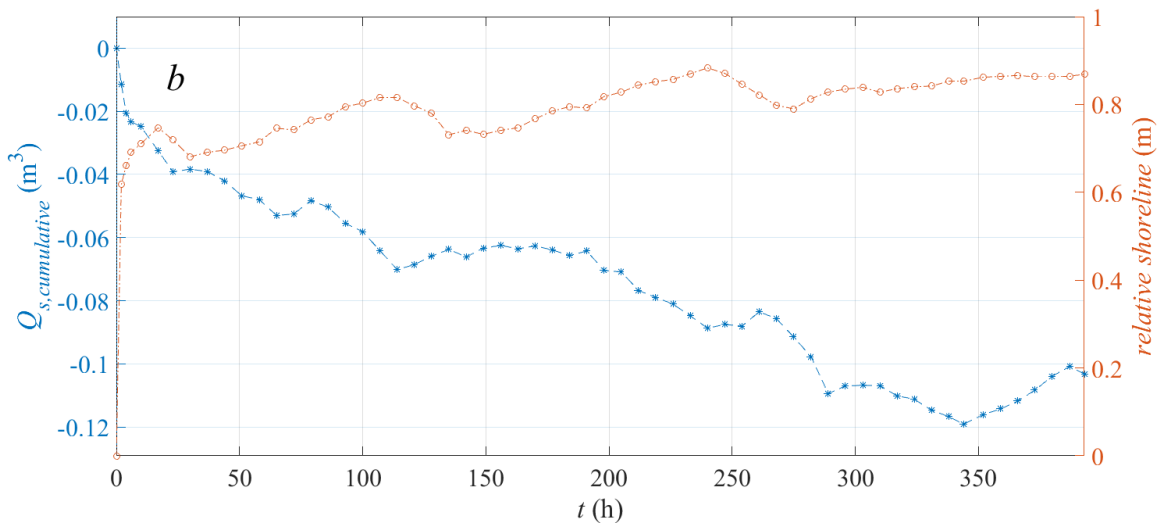
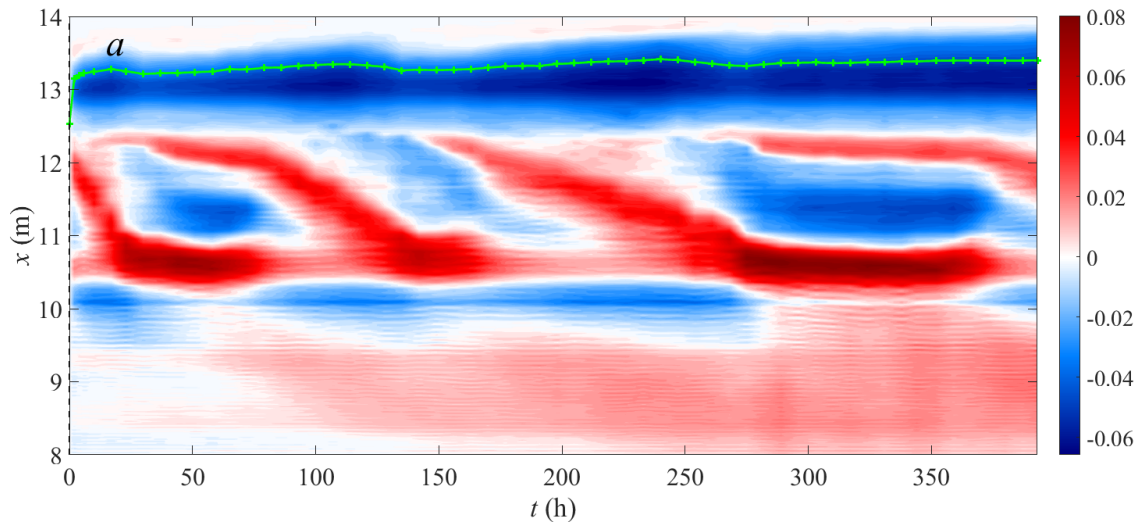
1014 Figure 6: Predicted versus observed recession of the shoreline for all experiments. Models predictions  
 1015 are identified by different markers: Original Bruun Rule (+), PTM (triangles) and Rosati et al.'s (2013)  
 1016 variant (squares). Solid, dotted and dashed lines indicate 0%, ±10% and ±30% error bounds,  
 1017 respectively.



1018

1019 Figure 7: Percentage error of each model with respect to the observed recession. Positive values indicate  
 1020 an over prediction.

1021



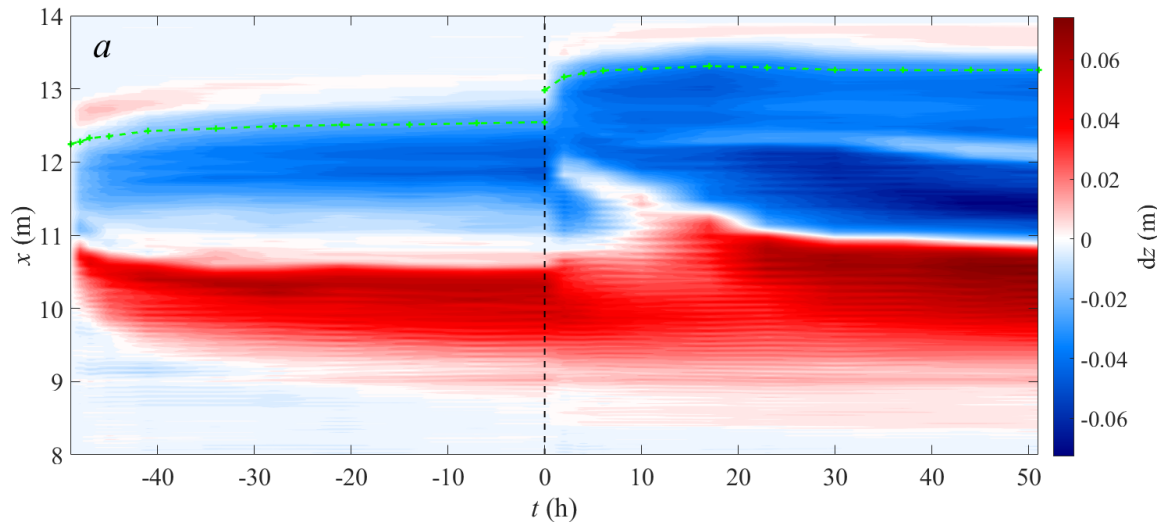
1022

1023

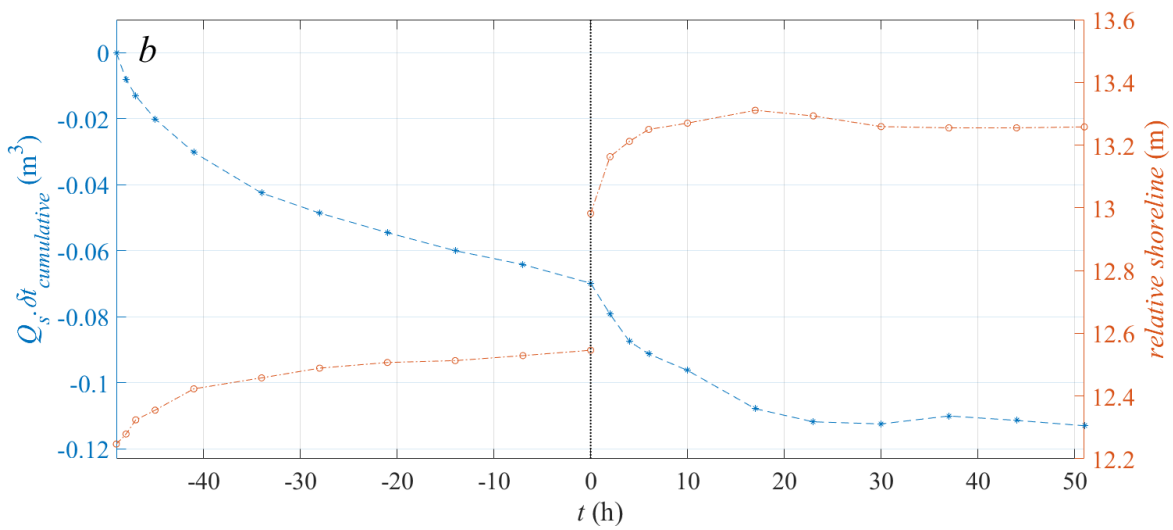
1024

1025 Figure 8: a) Contour plot of profile change versus time for Experiment E-1C. Colour bar in metres. The  
 1026 shoreline is indicated in green with + markers; b) Evolution of cumulative bulk transport,  $Q_s$ , and  
 1027 shoreline position versus time. Lower panels: Profile change and sediment transport ( $q_s(x)$ ) between two  
 1028 subsequent profiles during: c) the first bar decay sequence between  $t = 72$  h (blue dashed line) and  $t =$   
 1029  $79$  h (black solid line); and d) offshore bar propagation between  $t = 107$  h (blue dashed line) and  $t =$   
 1030  $114$  h (black solid line).

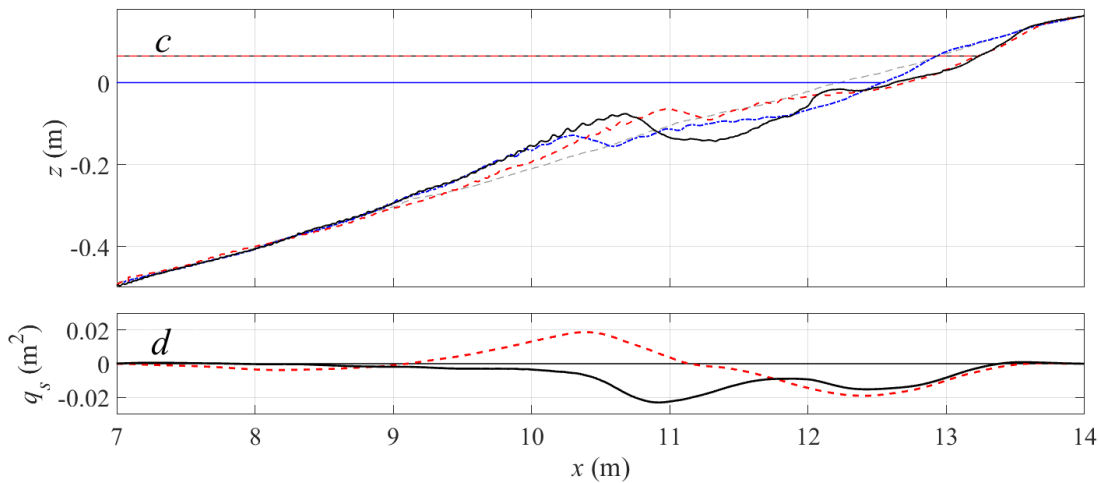




1031



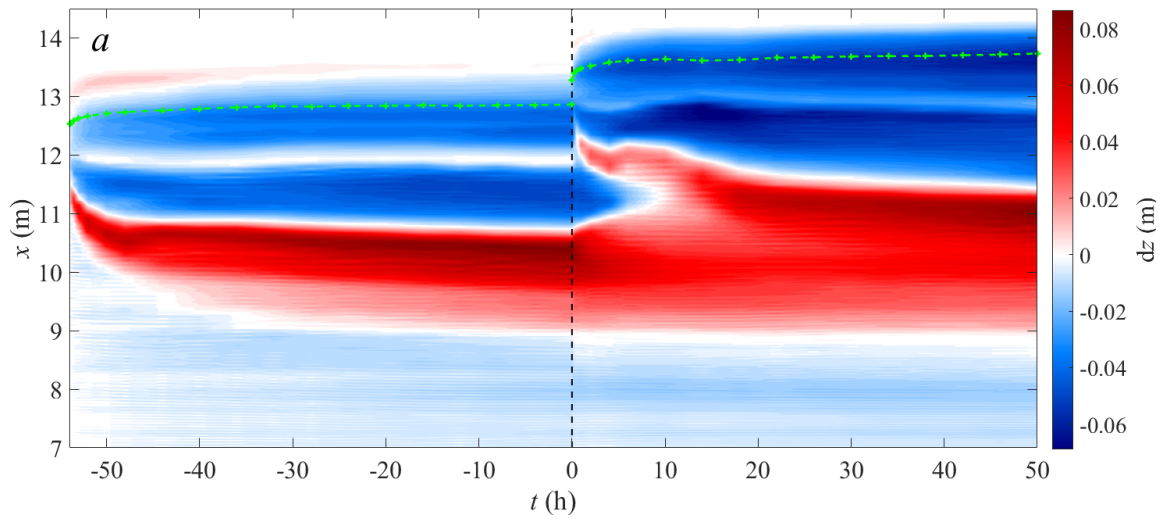
1032



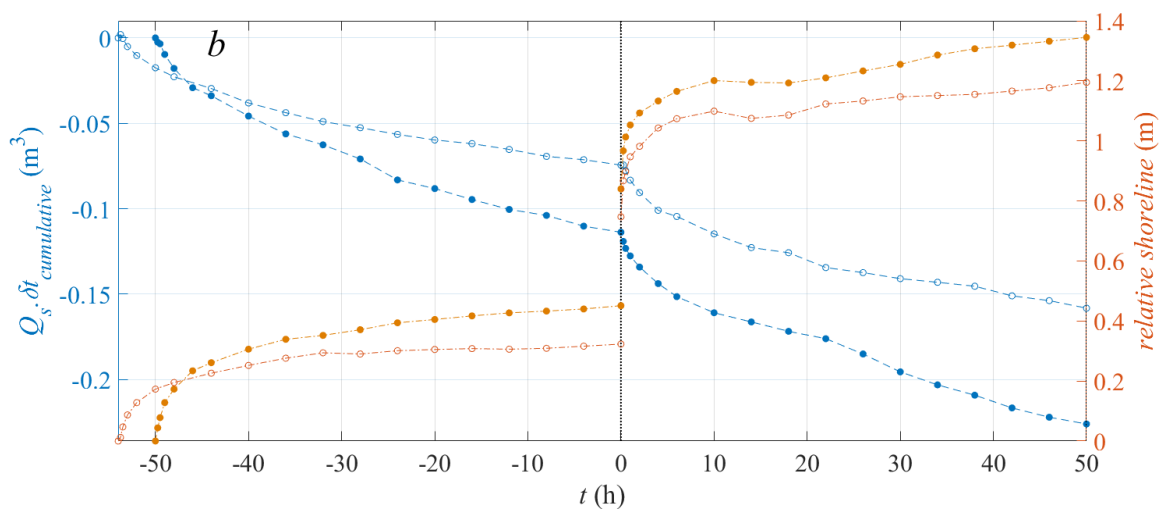
1033

1034 Figure 9: a) Contour plot of profile change versus time for Experiment E-1. Colour bar in metres. The  
 1035 shoreline is dashed green with + markers; b) Evolution of cumulative bulk transport,  $Q_s$ , and shoreline  
 1036 position versus time; c) Profile change between the initial planar profile (grey dashed line), final profiles  
 1037 at the initial (blue dashed line) and raised (black solid line) water level, as well as the translated initial  
 1038 water level profile using the PTM (red dashed line); d) Net sediment transport,  $q_s(x)$ , corresponding  
 1039 to the measured and translated profiles.

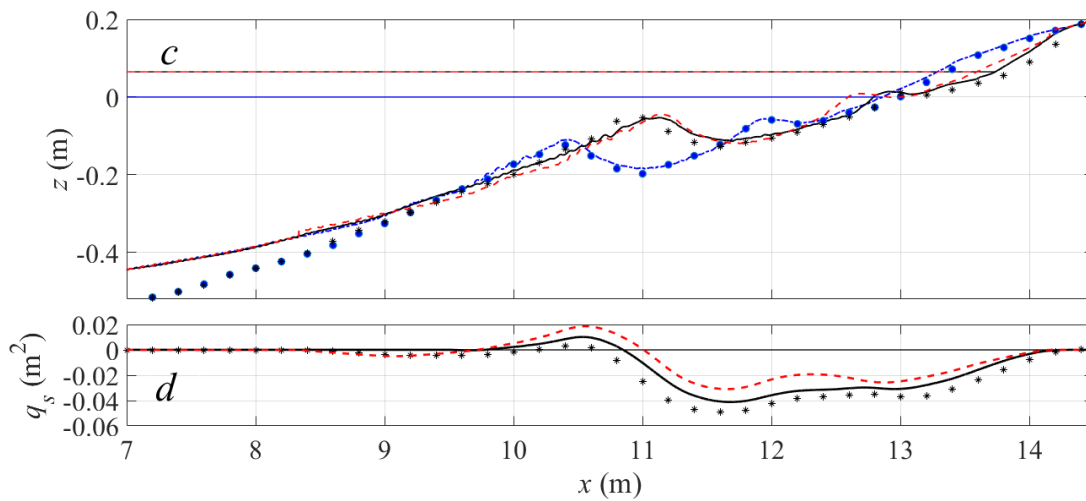
1040



1041

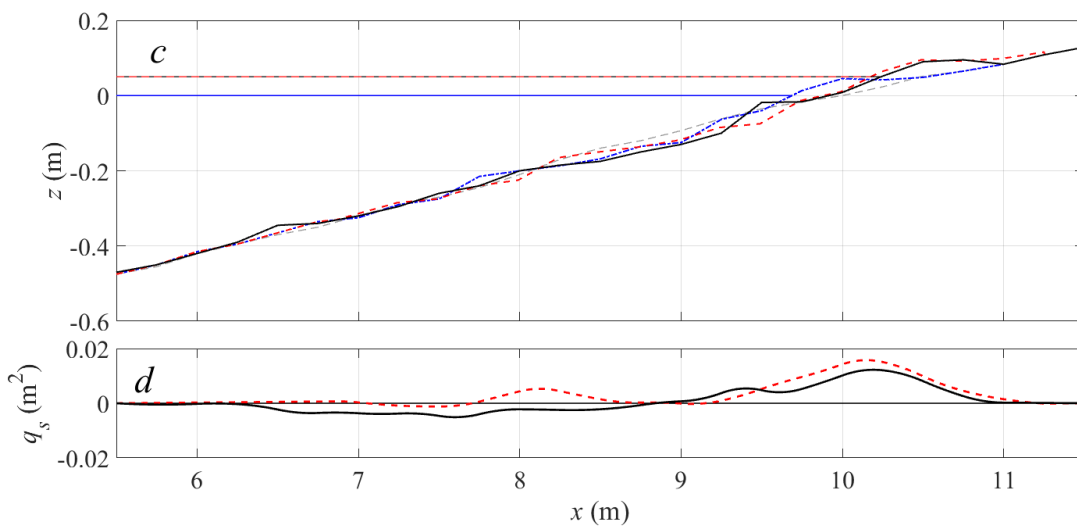
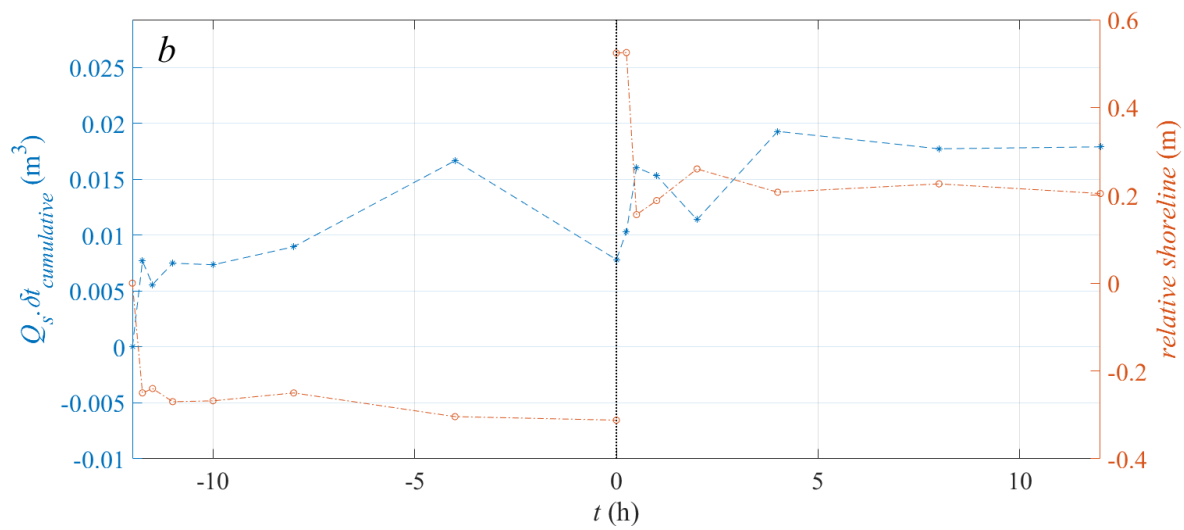
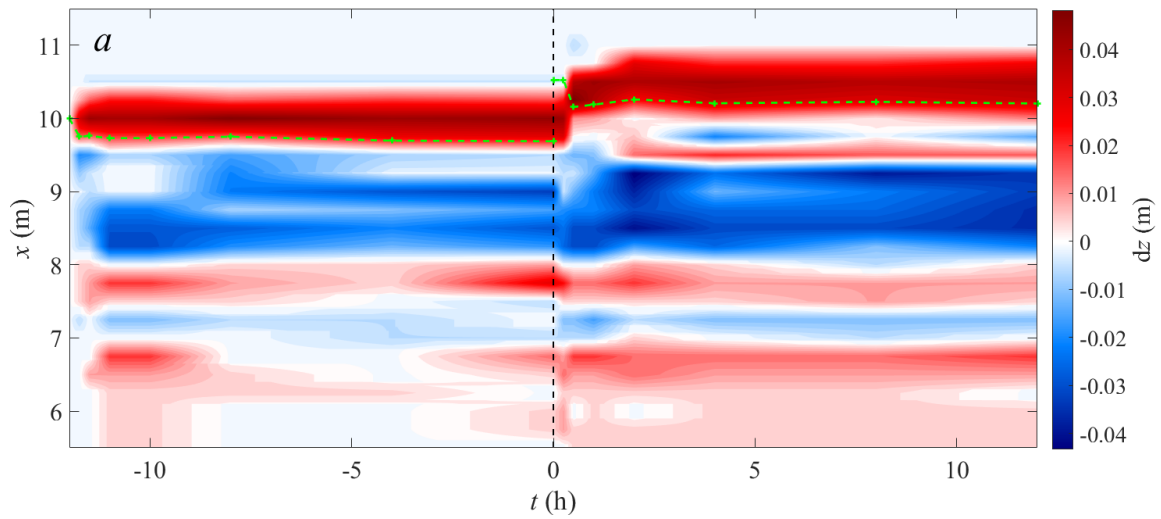


1042



1043

1044 Figure 10: a) Contour plot of profile change versus time for Experiment E-3. Colour bar in metres. The  
 1045 shoreline is dashed green with + markers; b) Cumulative  $Q_s$  (blue) and relative shoreline location  
 1046 (orange) before ( $t < 0$ ) and after water level rise for Experiments E-2 (filled circles) and E-3 (open  
 1047 circles); c) Observed and translated profiles for experiment E-3 showing final profiles at initial (blue  
 1048 dash-dot line) and raised (black solid line) water levels and PTM results (red dashed line); d) Net  
 1049 sediment transport,  $q_s(x)$ , corresponding to the measured and translated profiles. The final profiles  
 1050 before (blue dots) and after (black stars) water level rise and the net-transport distribution are also shown  
 1051 for Experiment E-2.

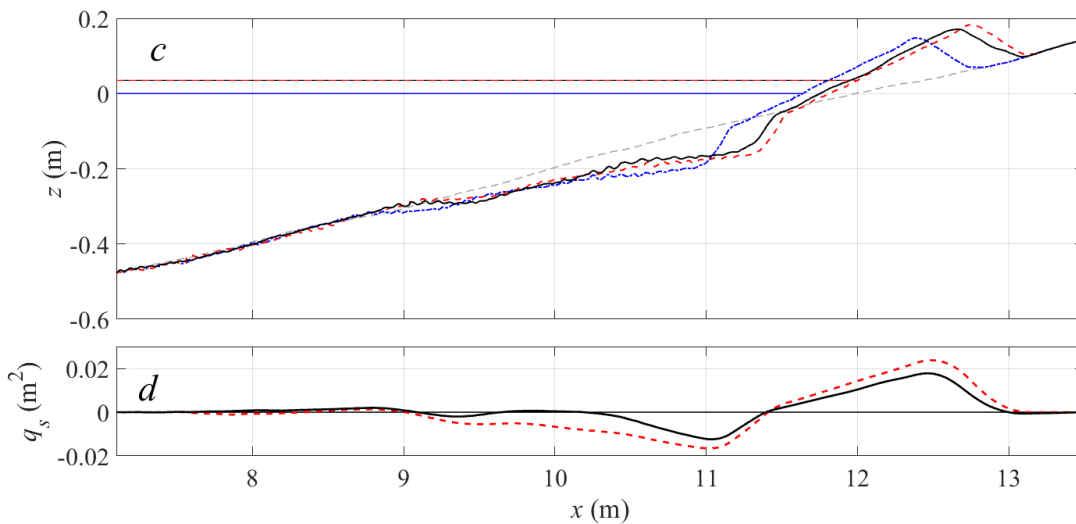
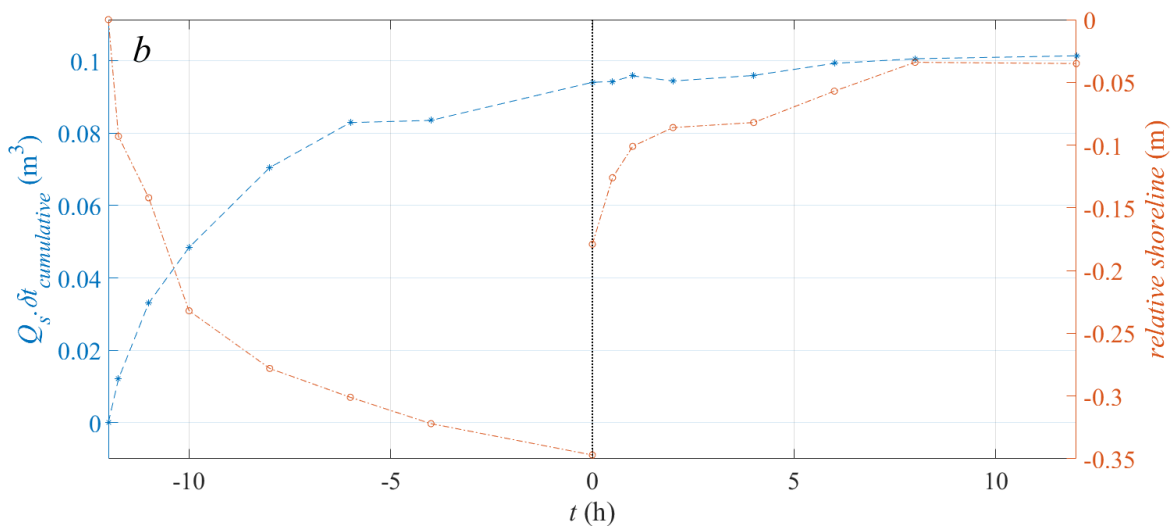
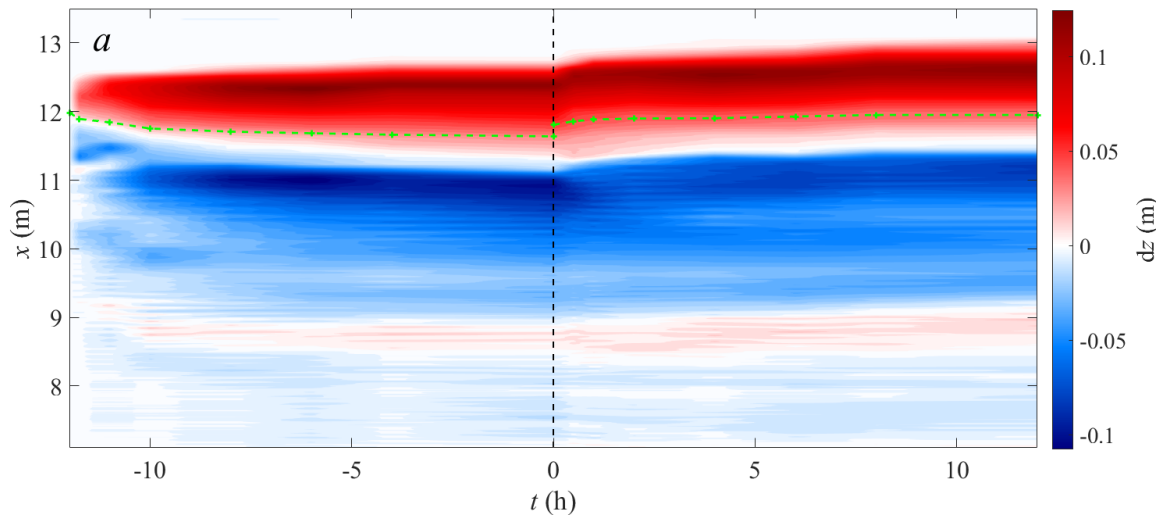


1052

1053

1054

1055 Figure 11: a) Contour plot of profile change versus time for Experiment A-1. Colour bar in metres. The  
 1056 shoreline is green with + markers; b) Evolution of cumulative bulk transport,  $Q_s$ , and shoreline position  
 1057 versus time; c) Profile change between the final profiles at the initial (blue dashed line) and raised (black  
 1058 solid line) water level as well as the translated initial water level profile using the PTM (red dashed  
 1059 line); d) Net sediment transport,  $q_s(x)$ , corresponding to the measured and translated profiles.

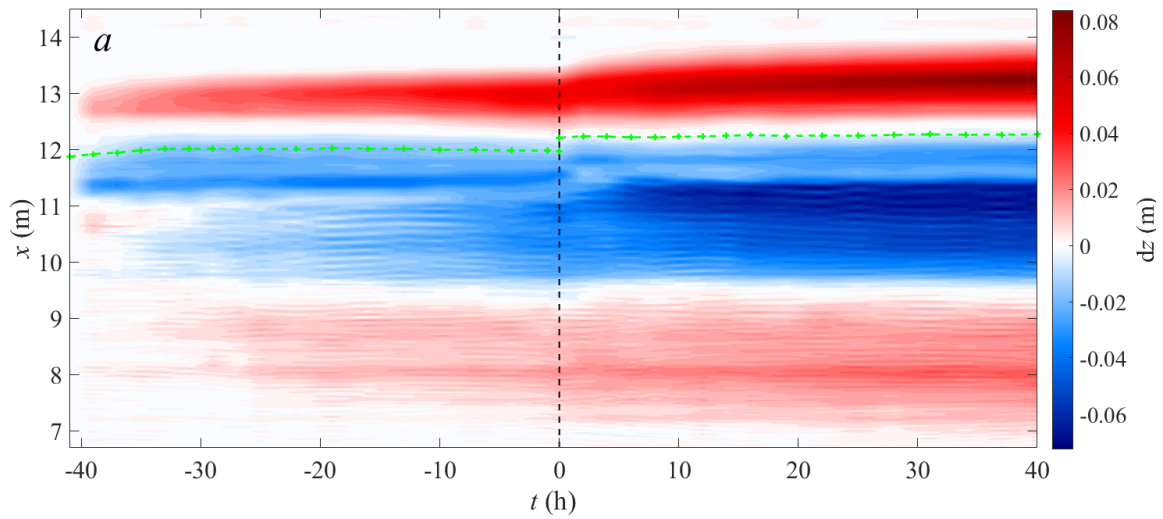


1060

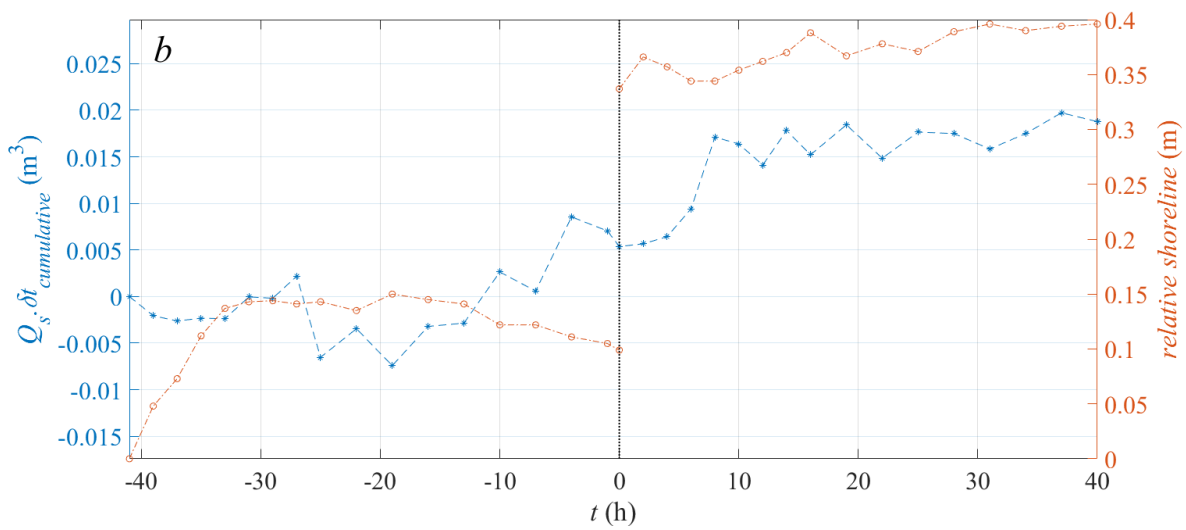
1061

1062

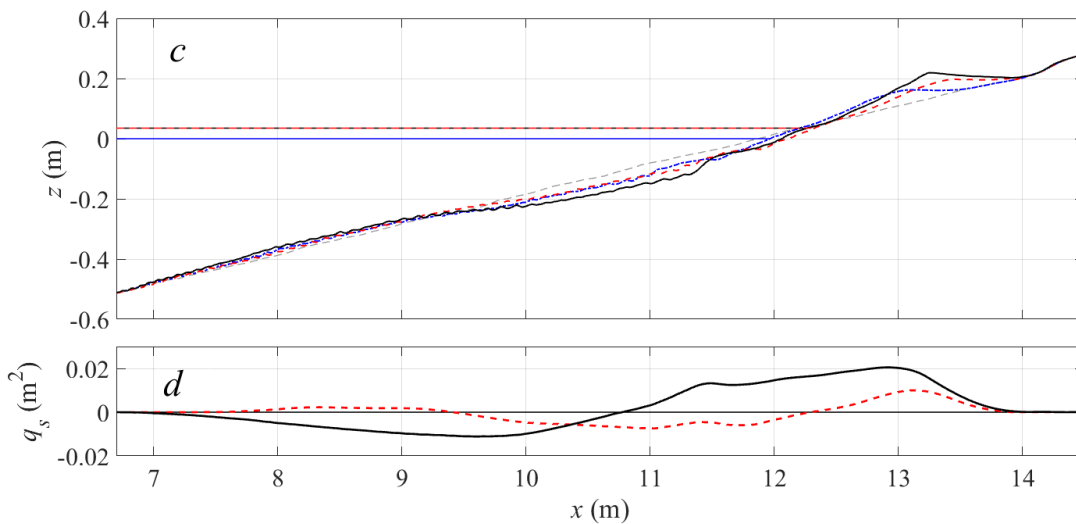
1063 Figure 12: a) Contour plot of profile change versus time for Experiment A-2. Colour bar in metres. The  
 1064 shoreline is green with + markers; b) Evolution of cumulative bulk transport,  $Q_s$ , and shoreline position  
 1065 versus time; c) Profile change between the final profiles at the initial (blue dashed line) and raised (black  
 1066 solid line) water levels as well as the translated initial water level profile using the PTM (red dashed  
 1067 line); d) Net sediment transport,  $q_s(x)$ , corresponding to the measured and translated profiles.



1068



1069



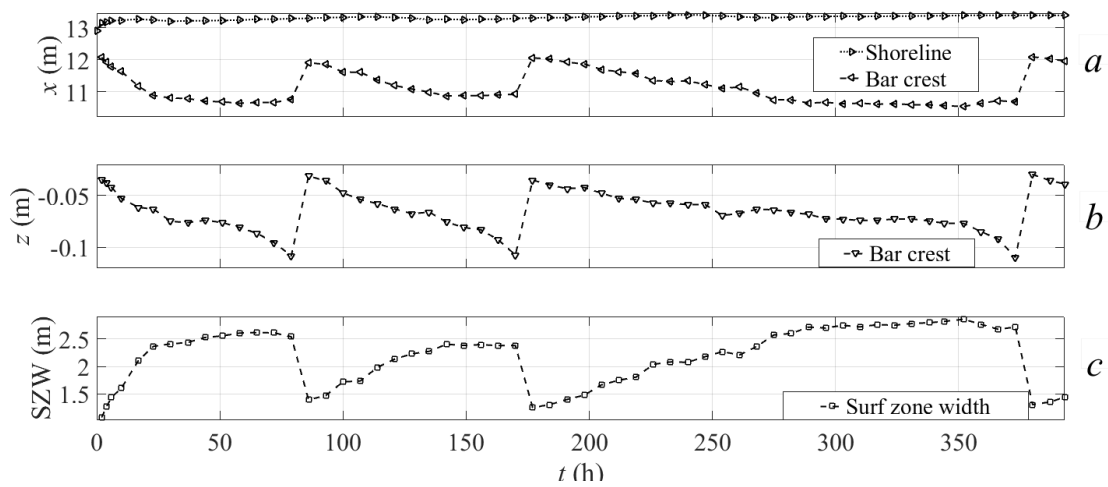
1070

Figure 13: a) Contour plot of profile change versus time for Experiment A-3. Colour bar in metres. The shoreline is green with + markers; b) Evolution of cumulative bulk transport,  $Q_s$ , and shoreline position versus time; c) Profile change between the final profiles at the initial (blue dashed line) and raised (black solid line) water level as well as the translated initial water level profile using the PTM (red dashed line); d) Net sediment transport,  $q_s(x)$ , corresponding to the measured and translated profiles.

1076

1077

1078

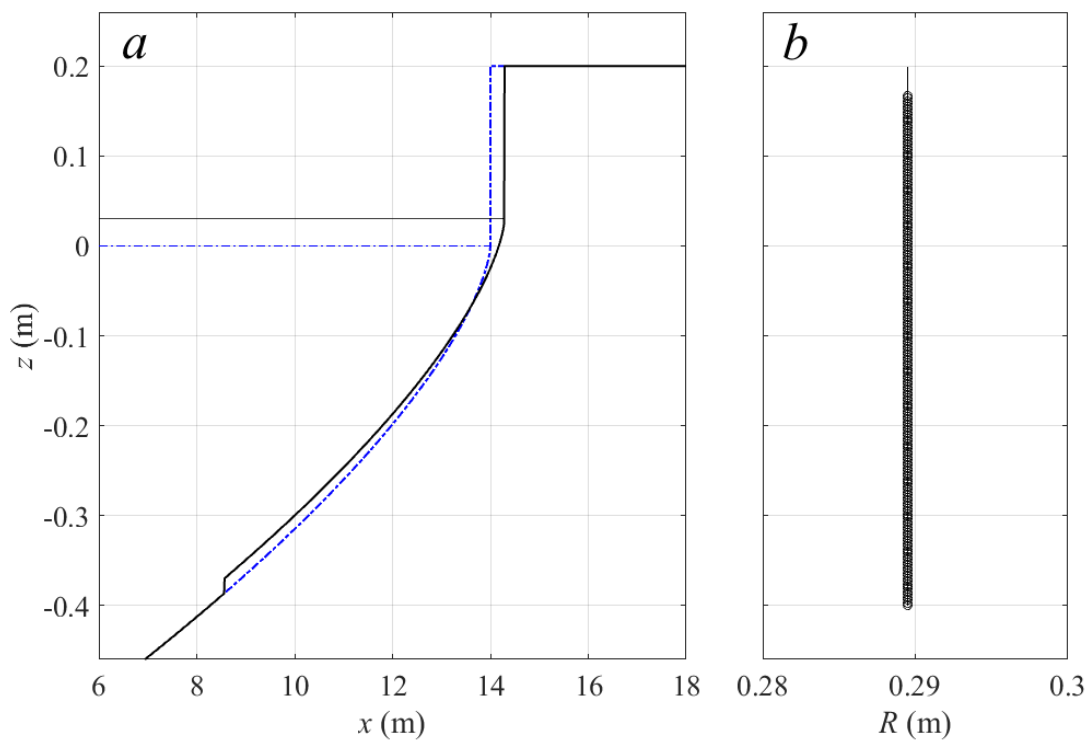


1079

1080

1081

Figure 14: Evolution of profile parameters over time for experiment E-1C. a) Shoreline and bar crest horizontal coordinate location, b) bar crest elevation and c) surf zone width ( $x_{shoreline} - x_{bar\ crest}$ ).

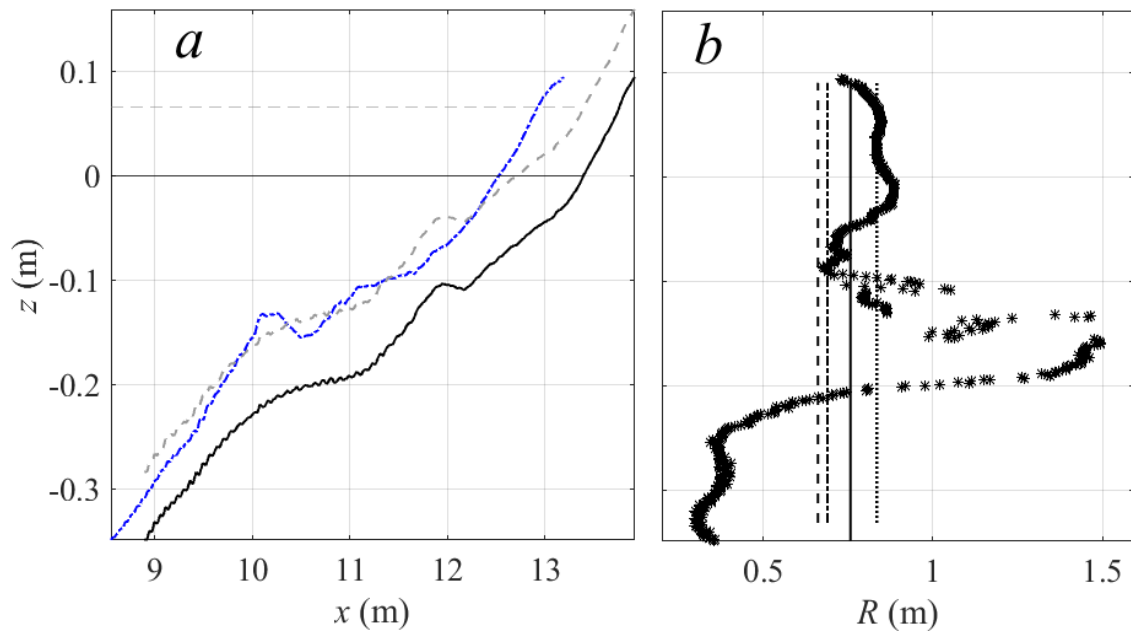


1082

1083

1084

Figure 15: a) Original and translated 2/3-power profile. b) recession at each contour,  $R(z)$ .

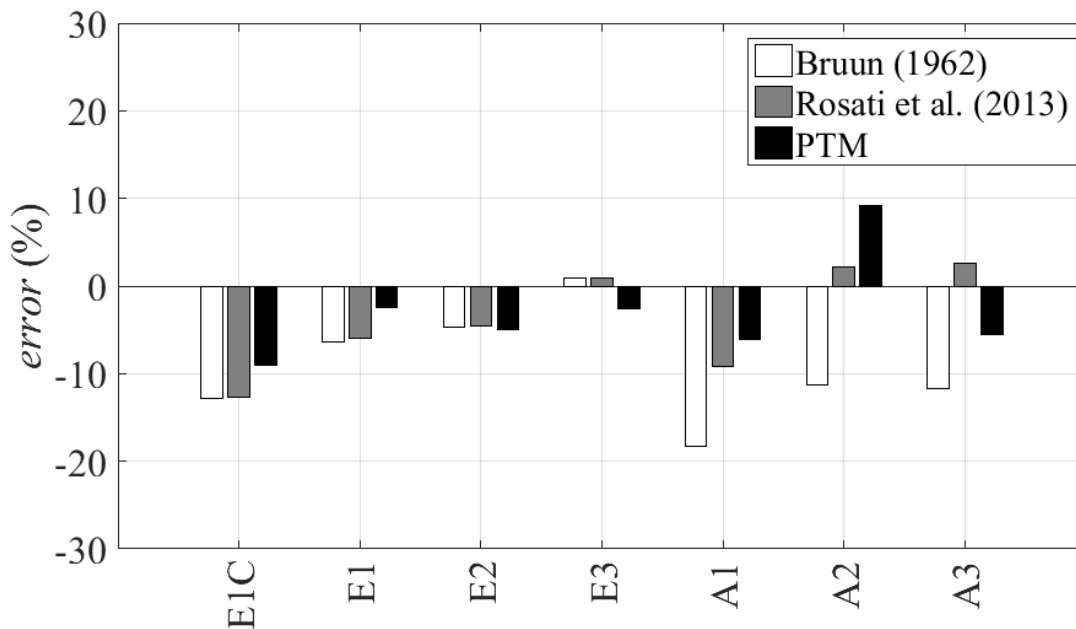


1085

1086

1087 Figure 16: a) Measured E-1C profiles: elevations of the final raised water level profile (dashed grey  
 1088 line) were reduced by -0.065 m (black solid line) to align with the final profile at the initial water level  
 1089 (blue dash-dot line). b) Each discrete contour recession is shown (black stars), along with the mean  
 1090 recession of the profile (solid line), Bruun Rule prediction (dashed line), PTM prediction (dash-dot line)  
 1091 and shoreline recession (dotted line) also indicated.

1092



1093

1094 Figure 17: Percentage error of each model with respect to the mean recession of the profile. The vertical  
 1095 axis scale is the same as Figure 9.